TECHNISCHE UNIVERSITÄT GRAZ

DIPLOMARBEIT

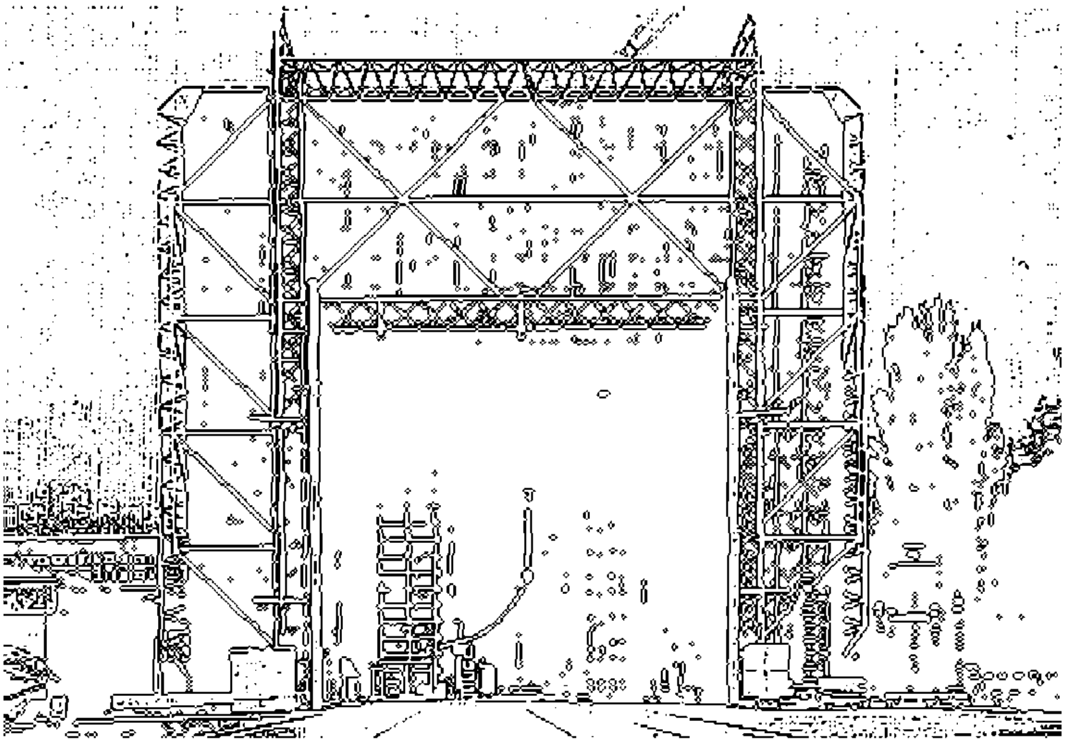

INSTITUT FÜR HOCHSPANNUNGSTECHNIK UND SYSTEMMANAGEMENT

Calculation of Thermal Capacitance and Magnetic Fields of Underground Power Cables with Finite Element Analysis Software

Berechnung thermischer Belastungen und magnetischer Felder für Hochspannungskabel mit der Finiten Elementen Methode

Diplomarbeit

vorgelegt von

Irena Vassileva

Graz, Sept. 2012

Durchgeführt am

Institut für Hochspannungstechnik und Systemmanagement der TU Graz

Institutsvorstand: O.Univ.-Prof.Dipl.-Ing.Dr.techn.Dr.h.c. Michael Muhr

Begutachter: Ao.Univ.-Prof.-Dipl.-Ing.Dr.techn. Rudolf Woschitz

Betreuer: Ao.Univ.-Prof.-Dipl.-Ing.Dr.techn. Rudolf Woschitz

Abstract

XLPE has become the worldwide preferred insulation material for high voltage power cables due to its high thermal stability, low dielectric losses and good aging properties. This allows XLPE power cables to transfer higher current during operation as well as under emergency and short circuit conditions. Since modern XLPE power cables come in different sizes, configurations and forms, it is important to choose the optimal underground power system to meet individual requirements, for example permissible current ratings, magnetic field regulations, power overloads, power losses, temperature increase, etc. Since these properties depend on factors like ambient temperature, physical soil characteristics, laying depth, etc. every cable installation must be calculated individually.

The finite element analysis program QuickField can easily be used for determining underground cable parameters. It is a very efficient and powerful FEA field calculation software package for the simulation of electromagnetic, thermal and mechanical stress; the modules can be combined in simulations. In this way, it is possible to optimise the thermal rating of a cable system depending on the requisite type of installation and laying depth according to the specified transmission capacity and prescribed limits for magnetic field strength. The results obtained with QuickField for permissible currents ratings at continuous load for buried cables in trefoil formation are compared to the results obtained using the IEC 60 287 standard.

QuickField offers visual feedback which makes it much easier to optimise cable design according to the specific requirements. Due to it simplicity of use, it is also a very good educational tool.

Keywords: XLPE power cables, permissible current ratings, magnetic fields, power losses, power overloads, temperature increase, soil physical characteristics, depth, finite element analysis, electromagnetic, thermal and stress design simulation.

Kurzfassung

Die kombinierende Wirkung einer hohen thermischen Stabilität, niedriger dielektrischen Verluste sowie der guten Alterungseigenschaften, kann mit dem weltweit eingesetzten Isolationsmaterial VPE für Hochspannungskabel erzielt werden. Eng damit verbunden bietet es die Möglichkeit im stationären Betrieb höhere Ströme zu führen und transiente Überlastungen stellen keine Gefährdung des Betriebes des Hochspannungskabels dar, sofern die zulässige Temperatur des Kabels nicht überschritten wird.

Mit dem heutigen Stand der Technik können VPE Kabelanlagen in verschiedenen Größen, Formen und Verlegearten gefertigt werden. Zur Erfüllung der individuellen Anforderungen, z.B. Belastbarkeit für Dauerbetrieb, Magnetfeld Grenzwerte, Überlastungen, Leistungsverluste, Temperaturerhöhung, etc., ist es wichtig das optimale Kabel zu wählen. Da diese Parameter von den Faktoren wie Geometrie vom Kabel, Materialeigenschaften der Kabelaufbauelemente, Umgebungstemperatur, Bodenaustrocknung und Verlegetiefe abhängen, muss jede Kabelanlagen individuell berechnet werden.

Das Programm QuickField, welches auf der Finiten-Elementen-Methode basiert, kann leicht zur Bestimmung verschiedener Parametern von Hochspannungskabeln verwendet werden. Es ist ein sehr effizientes und leistungsfähiges FEM Feldberechnungs-Softwarepaket für elektromagnetische, thermische und mechanische Belastungssimulation, welche miteinander gekoppelt werden können. Dadurch ist es möglich bei vorgegebener Übertragungsleistung und vorgeschriebenem Grenzwert für die magnetischen Feldstärke die thermische Auslegung einer Kabelanlage in Abhängigkeit der erforderlichen Verlegeart und Verlegetiefe zu optimieren.

QuickField bietet ein visuelles Feedback. Dies vereinfacht den Kabel-Entwurf nach den spezifischen Anforderungen zu optimieren. Die Berechnung der zulässigen Ströme im Dauerbetrieb bei Dreiecksverlegung eines Hochspannungskabels mit QuickField, werden mit den Ergebnissen unter Verwendung der Norm IEC 60 287 verglichen.

Schlüsselworte: VPE Hochspannungskabel, Belastbarkeit für Dauerbetrieb, Grenzwerte von magnetische Felder, Leistungsverluste, Überlastungen, Temperaturanstieg, Bodenaustrocknung, Verlegetiefe, Finiten Elementen Methoden, elektromagnetische, thermische und mechanische Belastungssimulation.

Table of Contents

1 Introduction....................3

2 XLPE Underground Cables Basic Design....................4

2.1 Conductor....................4

2.2 XLPE Insulation....................6

2.2.1 Advantages of XLPE Cables over Conventional Oil-Filled and PVC Cables....................7

2.3 Semiconducting Screens....................8

2.4 Metallic Screen....................9

2.5 Over Sheaths/Jackets....................10

3 Electric and Dielectric Losses....................11

3.1 Current Dependent Losses....................11

3.1.1 Conductor Losses....................11

3.1.2 Screen and Metallic Armouring Losses....................15

3.2 Dielectric Losses....................16

4 Thermal Model of Underground Power Cable....................19

4.1 Thermal Resistance Between One Conductor and the Sheath T1....................20

4.2 Thermal Resistance of Outer Insulation T3....................20

4.3 Soil Thermal Resistance T4....................21

4.3.1 Cable in flat formation with equal distance between the phases and equal losses:[12]..22

4.3.2 Cable in trefoil touching formation with equal losses:[12]....................23

5 Calculation of Underground Cable Carrying Capacity....................25

5.1 General....................25

5.2 Calculating Permissible Currents Ratings for Buried Cables Using IEC 60 287....................25

5.2.1 Buried AC cables where drying out of the soil does not occur....................25

5.2.2 Buried AC cables where the partial drying-out of the soil occurs....................26

5.2.3 Buried AC cables where the drying out of the soil is to be avoided....................27

6 Biological Effects of Alternating Magnetic Fields..28
6.1 General..28
6.2 Impact Mechanisms of Magnetic Fields on the Human Body...28
6.2.1 Eddy currents..28
6.2.2 Deflection of moving electrical charges [Lorenz force]..29
6.2.3 Resonance (hypothesis)..30
6.3 Acute Impacts..30
6.3.1 Stimulation of nerve and muscle cells...30
6.3.2 Resonances (mesomerism)...32
6.4 Limits for Alternating Magnetic Fields..32

7 QuickField Introduction..34
7.1 What is FEA?...34
7.2 Problem Description...35
7.2.1 AC Magnetic Analysis..35
7.2.1 AC Conduction Analysis...38
7.2.2 Thermal Analysis...40
7.3 How to Create A Model..42
7.3.1 Creating Model Objects..43
7.3.2 Meshing Technology..43
7.4 Coupled Problems..45

8 QuickField Implementation..47
8.1 Power Losses and Power Ratings of Solid and Stranded Conductors..................................48
8.1.1 Geometry of the Models...49
8.1.2 Required parameters...49
8.1.3 Results..50
8.2 Power Transfer Ratings for Cables in Different Formations with Solidly Earthed Screens ..52
8.2.1 Geometry and parameters of the model...52
8.2.2 Results..57
8.2.3 Discussion of results..58
8.3 Cables in Touching Trefoil and Flat Formation(1 and 2 Circuits) with Cross Bonded Screens

....58
8.3.1 Estimating the magnetic field above underground cables with QuickField..................58
8.3.2 Required parameters...58
8.3.3 Analysing the solution...59
8.3.4 Results...59
8.3.5 Discussion of the results..61
8.4 Estimating the Permissible Currents Ratings for Continuous Load......................................62
8.4.1 Results...67
8.4.2 Discussion of the results..68
8.4.3 Comparison of the results obtained with QuickField and IEC 60 287 standard for cable in trefoil formation...68
8.5 Calculating Transient Problems with QuickField...69
8.5.1 Required data...69
8.5.2 Results...71
8.6 Estimating the Power Transfer at Different Laying Depths for Single Trefoil Formation and Single Flat Formation...73
8.6.1 Required data...73
8.6.2 Results...73
8.6.3 Discussion of the results..74

9 Summary...75

10 Index...76
10.1 References..76
10.2 Symbols..78

1 Introduction

The increasing demand for electrical power due to urbanisation and industrial development has led to the need for the development of more reliable and efficient power transmission lines. Electric power is either transmitted using overhead lines or underground power networks. In urban areas, due to environmental, safety, aesthetic and other reasons, underground power systems are the preferred choice. There are also many old oil-filled underground power lines which need to be replaced by more efficient, reliable and environmentally friendly XLPE power systems. Since the costs for such installations are high, it is very important to use the optimal underground power lines that can meet the various requirement for urban areas such as prescribed magnetic fields limits, power overloads, etc.

The purpose of this paper is to test the different program modules of the finite element analysis package QuickField and to describe their application in calculating magnetic fields, permissible current ratings, thermal capacitance for transient loads and electric and dielectric losses for high voltage underground cables. The results obtained with QuickField for permissible current ratings at continuous load for buried cables in trefoil formation are confirmed using the results obtained using the IEC 60 287 standard. The simulation methods for calculating different cable system problems are described in detail in order to facilitate solving such problems for future QuickField users.

2 XLPE Underground Cables Basic Design

Depending on the specific requirements, XLPE power cables come in different sizes, materials and configurations. In general XLPE cables consist of the following components (see Figure 2.1):

- **Conductor** for current transfer
- **Semiconducting screens** for minimising the electrical stress around the conductor
- **XLPE insulation** for maintenance of the working voltage
- **Metallic screen** for neutralising the electric field outside the cable, draining capacitive and charging currents
- **Protective jacket** for mechanical, thermal, chemical and environmental protection of the cable [1]

Figure 2.1: XLPE cable design.[2]

2.1 *Conductor*

The conductor is used for current transfer and can be made out of copper (Cu) or aluminium (Al).

The use of copper is often preferred due to its significantly higher conductivity in comparison to aluminium (aluminium conductivity is 62 percent that of copper). For the same current ratings, a conductor made out of copper will have smaller cross-section and less power losses than a conductor made out of aluminium, but the temperature of the copper conductor will rise faster due to its smaller cross section.

One of the advantages of aluminium compared to copper is its lower costs. Another advantage is its lower density compared to copper – cables with aluminium conductors are half the weight of cables with copper conductors for the same current carrying capacity, in spite of the greater conductor cross section. [3]

In general cables with aluminium conductors are easier to handle. Problems which occur when using aluminium are due to its high thermal expansion coefficient and the formation of non conductive oxide layers in the conductor because of aluminium's affinity for binding with oxygen. [4]

The standard value for the specific resistivity of copper for conducting purposes at 20ºC, as specified by IEC 60 028, is ρ_{20}= 0.01724 $\Omega mm^2/m$ and the temperature coefficient is α_{20}= 3.93 10^{-3} K^{-1}. For aluminium the specific resistance specified by IEC 60 111 is ρ_{20}=0.028264 $\Omega mm^2/m$ and the temperature coefficient is α_{20}= 4.03 10^{-3} K^{-1}. [1]

Table 1 shows a comparison between the properties of aluminium and copper. The data is referenced to copper at 100. [3]

Table 1: Physical characteristics of aluminium and copper (data referenced to copper at 100) [3]

	Copper	Aluminum
Relative electric conductivity at 20ºC	100	62
Relative thermal conductivity	100	56
Tensile strength	100	51
Relative density	100	30
Relative thermal expansion coefficient	100	143

Figure 2.2 shows the different conductor shapes (round, oval and sector shaped) and the different conductor types (solid or stranded). Solid (single-wire) conductors are used for maximal utilisation of the conductor cross section and reduction of material usage. For conductors with big cross

sections, the bending forces increase. This is why cables with stranded (multi-wire) conductors are used. The conductor area is not solid so the conductor cross-section increases leading to higher insulation material usage. To counteract this problem, the stranded conductors are compacted. [1]

Another reason for using stranded conductors is to minimise the skin and proximity effects which occur when the conductor transfers alternating currents. These effects cause higher power losses due to the increased AC resistance in comparison to DC resistance. “Miliken” conductors are especially suitable for reducing the AC/DC ratio. They consist of a collection of shaped stranded conductors, lightly insulated from each other (see Figure 2.2 d). [3]

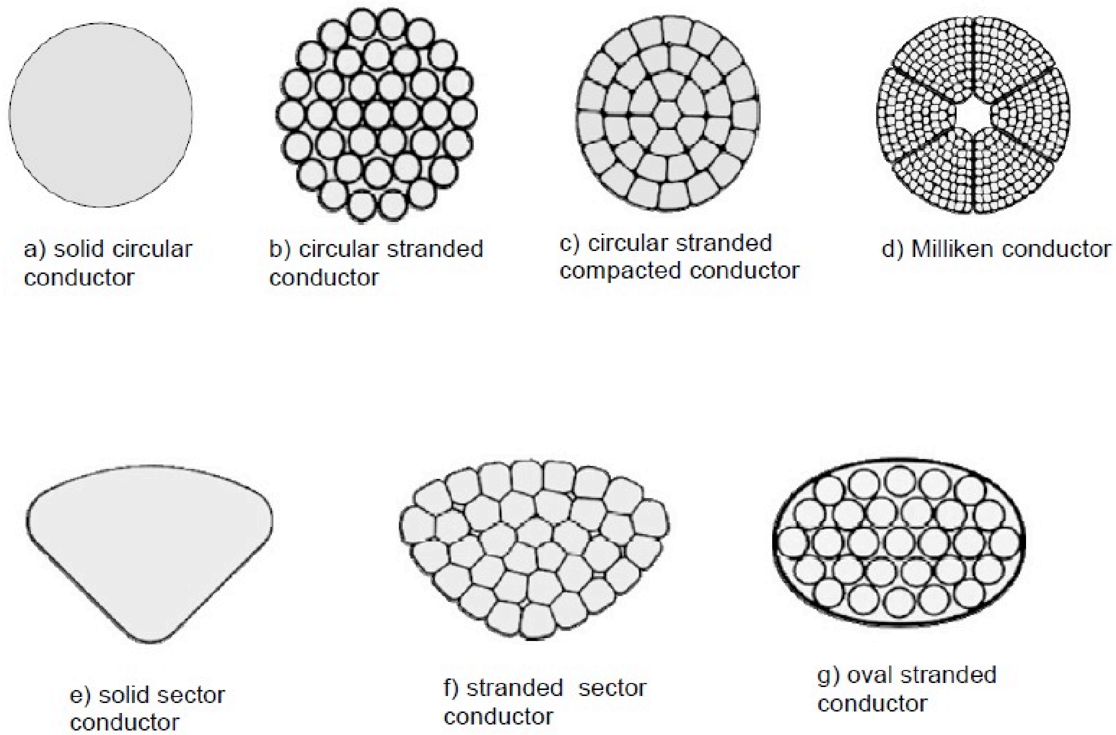

Figure 2.2: Conductor forms [6]

2.2 *XLPE Insulation*

The purpose of the insulation is to insulate the current carrying conductors from each other and from the metallic screen. Cross-linked polyethylene (XLPE) contains three-dimensional cross linked bonds in the structure of the polymer, changing it from a thermoplastic to a thermoset material. This bonds improve the thermal, chemical and physical properties of the polymer. There are three methods for producing XLPE:

- Peroxide method
- Silane method
- Electron-beam processing method [1]

2.2.1 *Advantages of XLPE Cables over Conventional Oil-Filled and PVC Cables*

XLPE has higher resistance to thermal deformation, higher resistance to chemicals, better aging properties and increased impact and tensile strength compered to older insulation materials like PVC and oil/paper. Other advantages of XLPE compared to older insulation materials are its lower dielectric constant and its ability to endure higher conductor temperatures during standard and emergency operations, allowing for higher current and power ratings. XLPE cables allow the maximum conductor temperature to be 90ºC at continuous load and 140ºC for emergency conditions. Under short circuit conditions, the temperature can reach 250ºC. For these reasons, XLPE cables can handle larger currents compared to the older systems. Table 2 shows some of the electrical and physical properties of different cable insulation materials.

Table 2:Properties of cable insulation [5]

	Oil/paper	PVC	PE	XLPE
Dielectric Loss Factor tanδ at 20 ºC, 50Hz	3×10^{-3}	50×10^{-3}	$>0.3\times10^{-3}$	$>0.3\times10^{-3}$
Dielectric Constant ε_r at 20 ºC, 50Hz	3.5	5	2.3	2.3
Volume Resistivity [Ω.cm]	$\sim10^{15}$	$\sim10^{15}$	$>10^{16}$	$>10^{16}$
Operating Temperature Rating [ºC]	55...65	65...70	70	90

The list below summarises the advantages of XLPE cables compared to older oil-filled and PVC systems: [5]

- Less dielectric losses
- Lower charging currents
- Lower earth leakage currents
- Higher current/power ratings

- Higher emergency overload ratings
- Higher short circuit ratings
- Higher insulation resistance
- Excellent moisture penetration resistance
- Excellent resistance to chemicals
- Lower weight
- Smaller banding radius
- Easier installation
- Minimal maintenance cost
- Better environmental compatibility (no oil leakage)

2.3 *Semiconducting Screens*

The extrusion of semiconducting screen over the conductor and the insulation is done in order to assure a cavity free connection between the insulation and the conductors, metallic screens and the protective jacket. It also reduces the border field strength and provides homogenous electric field around the conductors, ensuring that the electric field stays within the cable core as shown in Figure 2.3. Semiconducting screens are made out of conducting polymers or semiconducting tapes. [7]

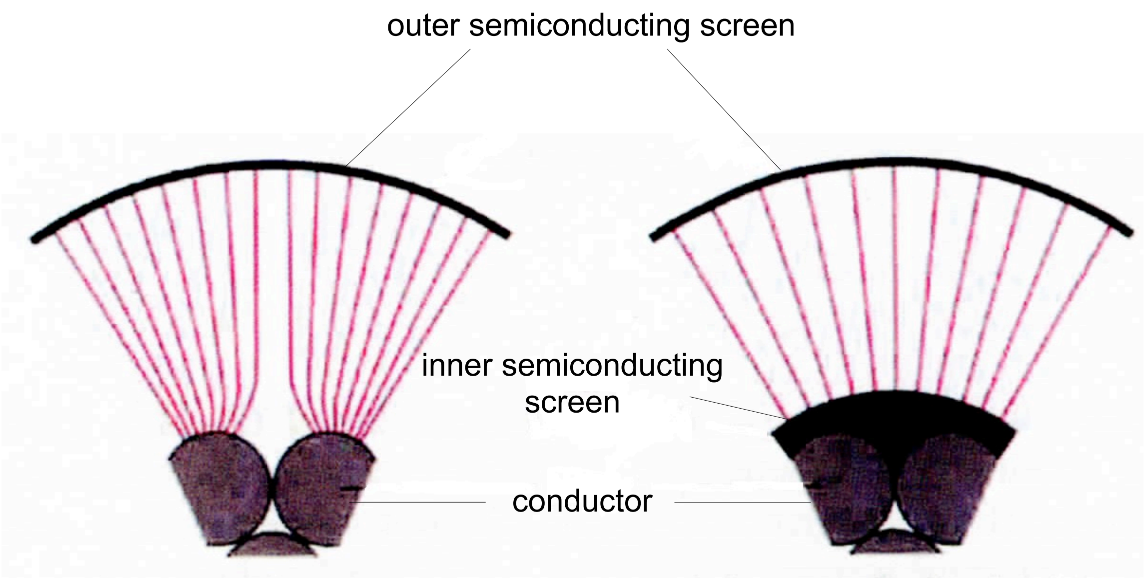

Figure 2.3 : Outer and inner semiconducting screens [7]

The conductor screen also smooths out the surface irregularities of the conductor strands. The materials for the semiconducting screens must be compatible with both the insulation and the conductor. [3]

Good electrical long-term stability for thick-walled insulation requires high purity of the insulation compounds as well as a stable, strong, homogenous connection between the insulation and the semiconducting layer. The so-called triple extrusion method developed by Siemens in the sixties meets these requirements.

Through this manufacturing method, the extrusion of the inner semiconducting screen, the insulation and the outer conducting screen is done simultaneously using a triple extrusion head over the conductor, pre-heated to 100°C, and this is then cross-linked together. [7]

2.4 *Metallic Screen*

The metallic screen has the following purposes: [7]

- To keep the insulation screen at ground potential
- To drain capacitive, leakage, charge and fault currents
- For electric shock protection

The metallic screens surround the cable core and have a wide range of configurations: thin tapes, extruded tubes, longitudinally welded metals, extruded and corrugated metals, etc. The materials used for the metallic screens are lead, aluminium, stainless steal and copper. Metallic screens must have good galvanic contact with the insulation screen. If the contact is insufficient, it can lead to potential difference between the metallic screen and the insulation screen, causing discharges which could deteriorate the screen and could cause cable failure. [3]

2.5 *Over Sheaths/Jackets*

The last layer of the cable is a protective jacket which can be made out of metal or polymer. The metals used for the protective jacket are lead or aluminium and the polymers are PVC, PE, LDPE, MDPE, HDPE or nylon. The purpose of the protective jacket is to provide additional electrical, thermal, mechanical, chemical and environmental protection for the enclosed cable, extending the life of the cable.

Jackets can be extruded, pressed, annular, encapsulated or overlaid. In order to stop water penetration into the inner layers of the cable, the space under the jacket is sometimes filled with absorbent polymer. [3]

3 Electric and Dielectric Losses

During the transfer of electrical energy (product of applied current and voltage) through underground cables, different types of losses occur in its component parts. Current dependent losses occur in the metallic components of the cable and voltage dependent losses occur in the non-metallic components of the cable. Since current dependent losses represent a big portion of the total power loss, in order to transfer energy with less losses the current must be low and the voltage high.

Current dependent losses (electric losses) are Joule losses in the conductors, circulating currents or induced losses (eddy currents) in the metallic screens and armouring. Voltage dependent losses, also known as dielectric losses, are induced by alternating electric fields in the cable insulation. Both electric and dielectric losses are transformed into heat.

These losses can be calculated with the formulas in the IEC publication 60 287 (Electric Cables -Calculation of the Current Rating – Part 1: Current rating equations and calculating of losses) or with a finite element analysis application like QuickField.

In this theses the calculations are done for 500kV single core XLPE cables in different formations (flat and trefoil) and at different depths.

3.1 *Current Dependent Losses*

Current dependent losses can be divided into conductor losses, screen losses and losses which occur in the metallic armouring and pipes.

3.1.1 *Conductor Losses*

Electric losses occur in the form of heat during the transmission of electric current through the conductor. The electric current is a flow of charges (electrons), and these moving charges collide with the fixed ions of the metal lattice causing the lattice ions to vibrate and dissipate energy as heat. This process depends on the degree of the metal resistance and on the current flow and is called Joule heating. James Pascott Joule was the first to study this process in 1941. He experimented with a wire carrying a known current immersed in a fixed volume of water for a 30 minutes period and measured the temperature rise of the water. By changing the wire length and the current flow in the wire, he concluded that the heat produced in the wire by the applied current is proportional to the square of this current multiplied by the electric resistance of the wire (Joule's first law). [8]

A metal's AC resistance is higher than its DC resistance due to skin and proximity effects which occur when an alternating current passes through the conductor.

- *Skin effect*

The cause for the skin effect is the occurrence of alternating magnetic field around the conductor during the passage of alternating electric current through the conductor. In turn this alternating magnetic field induces eddy currents in the conductor which overlay the current passing through the conductor. In Figure 3.1 one can see that the current density is high in the outer regions of the conductor and lower in the centre of the conductor because the eddy currents have the same direction as the source current near the outer region and the opposite direction in the centre of the conductor. [9]

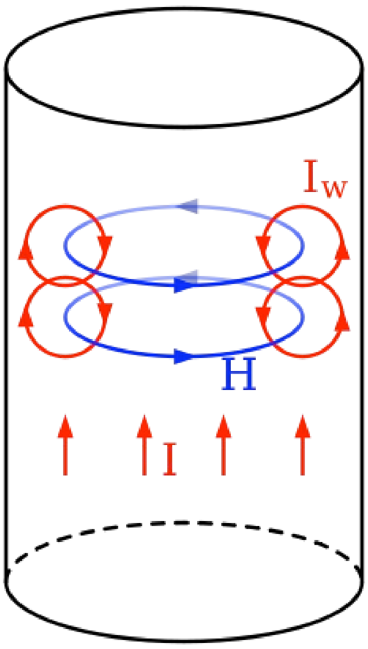

Figure 3.1: Skin effect [9]

Due to the skin effect, the useful conductor area is reduced, increasing the effective conductor resistance.

The skin effect depends on the conductor design, cross-section, its material resistivity and the frequency of the applied current. The skin effect factor y_s summarises these influences. [10]

The skin effect factor is given in the IEC publication 60 287 [11]:

$$y_s = \frac{x_s^4}{192 + 0.8 \times x_s^4} \tag{3.1}$$

where

$$x_s^2 = \frac{8 \times \pi \times f}{R'} \times 10^{-7} \times k_s \tag{3.2}$$

f	supply frequency [Hz]
x_s	argument of Bessel function used to calculate skin effect
k_s	skin effect coefficient
R'	conductor DC resistance at maximum operating temperature [Ω/m]

The above formula is accurate when x_s does not exceed 2.8, and therefore applies to the majority of practical cases. Values for k_s are given in Table 3.1. [11]

- *Proximity effect*

The proximity effect is another magnetic effect caused by the proximity of the conductors in a three-phase system. This time the current density of the conductor becomes non-homogeneous because the current seeks to concentrate in current paths as far away as possible from the distributing neighbour due to eddy currents induced by this neighbour in the conductor. This effect makes the conductor areas close to the neighbour less useful for transporting current. For closely spaced conductors with big current carrying capacity, this effect is more prominent. [10]

The proximity effect factor for triple core cables and for three single core cables with circular conductors is given in the IEC publication 60 287 formula [11]:

$$y_p = \frac{x_p^4}{192+0.8\times x_p^4}\times\left(\frac{d_c}{s}\right)^2\times\left[0.312\times\left(\frac{d_c}{s}\right)^2+\frac{1.18}{\frac{x_p^4}{192+0.8\times x_p^4}+0.27}\right] \quad (3.3)$$

where

$$x_p^2 = \frac{8\times\pi\times f}{R'}\times 10^{-7}\times k_p \quad (3.4)$$

x_p argument of Bessel function used to calculate proximity effect

d_c diameter of conductor [mm]

s distance between conductor axes [mm]

k_p proximity effect coefficient

From formulas 3.3 and 3.4, it is easy to recognise that the proximity effect factor depends on the cable design, the conductor resistivity, the conductor cross section, the conductor type and the frequency of the applied current.

The above formula is accurate when x_p does not exceed 2.8, so it applies to the majority of practical cases. Values for k_p are given in Table 3.1. [11]

Table 3.1 *Skin effect and proximity effect coefficients [11]*

Type of conductor	**Dried and impregnated**	**k_s**	**k_p**
Round, stranded	Yes	1	0.8
Round, stranded	No	1	1
Round, compact	Yes	1	0.8
Round, compact	No	1	1
Round, segmental	-	0.435	0.37
Sector-shaped	Yes	1	0.8
Sector-shaped	No	1	1

The resulting resistance of the conductor loaded with alternating current at maximum operating temperature is given with this formula:

$$R_{AC} = R' \times \left(1 + y_s + y_p\right) \quad (3.5)$$

R_{AC} conductor AC resistance at maximum operating temperature [Ω/m]

R' conductor DC resistance at maximum operating temperature [Ω/m]

y_s skin effect factor

y_p proximity effect factor.

The conductor DC resistance R' can be calculated with the following formula:

$$R' = R_0 \times \left[1 + \alpha_{20} \times \left(\Theta - 20\right)\right] \quad (3.6)$$

R_0 conductor DC resistance at 20°C [Ω/m]

α_{20} temperature coefficient of electrical resistance at 20°C

Θ maximum operating temperature [ºC]

For calculating the conductor losses, the AC resistance R_{AC} is used. For conductors with small cross sections (<500mm^2) the skin and proximity effect increase the effective AC resistance of the conductor by less than 10%. For conductors with very big cross sections (>2000mm^2), skin and proximity effects can increase the AC resistance by more than 30%. [10]

3.1.2 *Screen and Metallic Armouring Losses*

The metal elements of the cable (screens, armouring and metallic protection pipes, if applied) also contribute to the current dependent losses; the total current dependent losses are described with the formula below [10]:

$$P_i = n \times I^2 \times R_{AC} \times \left(1 + \lambda_1 + \lambda_2\right) \quad (3.7)$$

P_i total current dependent losses per m [W/m]

I	applied current [A]
n	number of conductors
R_{AC}	conductor AC resistance at 90ºC [Ω/m]
λ_1	loss factor of the metallic screen
λ_2	loss factor of the metallic armouring and pipes

The induced eddy and circulating currents in the metallic screen and armouring, due to the alternating magnetic field around the conductor and the alternating current passing through the conductor, contribute to heat generation and therefore a reduction in the cable ampacity.

The losses in the metallic screen λ_1 depend on its electric resistance, its inductance and the phases arrangement in relation to each other. For trefoil formation, the loss factor of the metallic screen is much lower than for a flat formation because the magnetic fields around the conductors cancel each other out to some extend. When the screen is grounded on both sides, circulating currents occur in it causing considerable reduction in cable ampacity. In order to reduce these losses, the screens of underground power cables are often cross-bonded or single-side bonded. Eddy currents generated in the screen by the alternating conductor current can be ignored since they are much smaller than the circulating currents in the screen when the screen is grounded on both sides. [10]

The loss factor of metallic armouring and pipes λ_2, if applied, depends on the material they are made of and are mostly affected by eddy currents. In particular steel wire armouring is affected by these currents because the magnetic properties of the material attract and concentrate the magnetic induction. Both loss factors are expressed as a factor relating the losses to the conductor losses. [10]

3.2 *Dielectric Losses*

High voltage power cables are in effect elongated cylinder capacitors with capacitance per unit length C. This capacitance depends on the insulation material, thickness and on the conductor cross section. [7]

The dielectric losses as mentioned earlier transfer into heat and also contribute to a decrease in cable ampacity. The dielectric insulation material of the cable can be represented as combination of resistance and capacitance connected in parallel between the conductor and the grounded screen. This explains the occurrence of capacitive and resistive current when a voltage is applied to the conductor.

Figure 3.2 represents a vector diagram of the applied voltage and the resulting resistive and capacitive current. One can see that the resistive current is in phase with the applied voltage, while the capacitive current is shifted by 90°. The resistive current contributes to the losses of the cable. The loss tangent angle tan δ is a dielectric material parameter and is expressed by the ratio between resistive and capacitive current [10]:

$$\tan\delta = \frac{|I_R|}{|I_C|} = \frac{1}{(R_i \times C \times \omega)} \qquad (3.8)$$

R_i resistance of a 1 m piece of cable insulation [Ω/m]

ω angular frequency of the AC voltage $\omega = 2 \times \pi \times f$ [Hz]

C cable capacitance per unit length [µF/km]

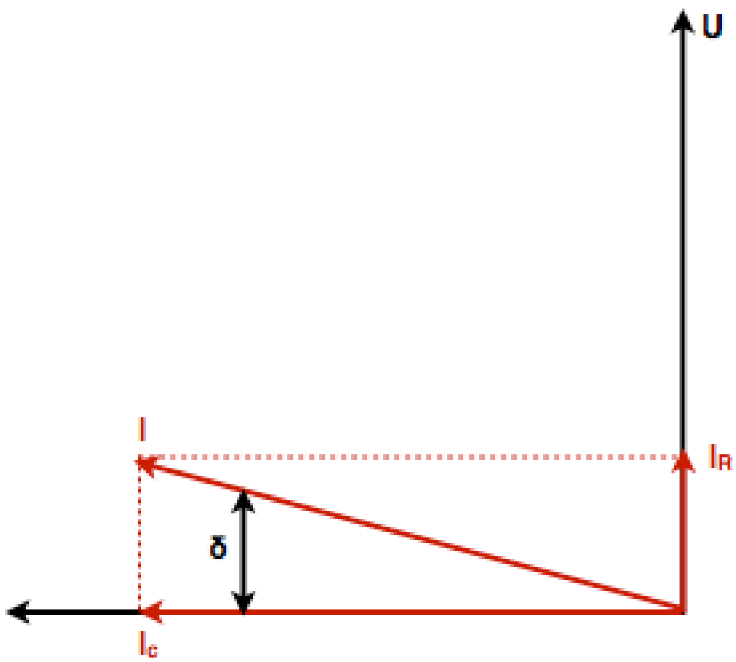

Figure 3.2: Loss tangent diagram [6]

The cable capacitance per unit length C [F/m] is given by:

$$C = \frac{\varepsilon}{18 \times \ln\left(\frac{D_i}{d_s}\right)} \times 10^{-9} \quad (3.9)$$

D_i diameter of the insulation [m]

d_s diameter of the conductor screen [m]

ε dielectric constant of the insulation material (Table 2)

The dielectric losses of the insulation per phase is given by [11]:

$$W_d = \omega \times C \times U_0^2 \times \tan\delta \quad (3.10)$$

W_d dielectric losses per phase [W/m]

U_o the voltage to earth [V]

Since the dielectric losses increase with the square of the cable voltage, they are relevant only at high voltage levels. According to IEC 60 287, they can be ignored for XLPE cables under 127kV. [10]

4 Thermal Model of Underground Power Cable

The losses which occur in power cables during transmission of electricity as mentioned earlier are transformed into heat. These heat is transferred through the thermal resistance of the insulation and the protective jacket to the cable surface, from there the heat dissipates through the soil to the ground surface and then into the surrounding environment. This is quantified by the soil thermal resistivity. In equilibrium (steady state condition) the dissipated heat is the sum of all losses in the power cable.

Using the analogy between heat flow Φ and electric current I, the following thermal equivalent circuit of underground power cables can be used in order to show the heat dissipation. The thermal resistance of the cable and the thermal resistance of the soil are connected in series (see Figure 4.1).

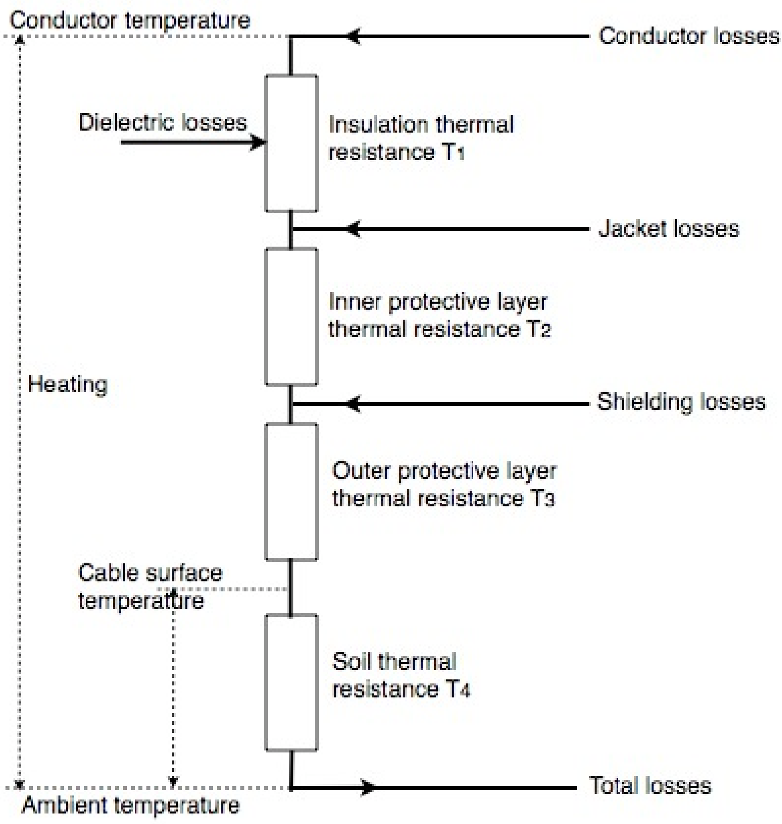

Figure 4.1: Thermal equivalent circuit for underground cable [6]

The low for the heat flow is analogous to the Ohm's low, wherein heat flow is equivalent to the electric current, the conductor temperature rise is equivalent to voltage, the sum of absolute thermal resistance is equivalent to electric resistance R.

$$U = I \times R \qquad (4.1)$$

$$\Delta\Theta_C = \Phi \times \Sigma T \qquad (4.2)$$

The heat flow Φ is sum of losses induced by the current and the voltage in the cable.[6]

The calculation of the thermal resistance can be done using the formulas from IEC publication 60 287.

4.1 *Thermal Resistance Between One Conductor and the Sheath T_1*

The thermal resistance between one conductor and the sheath T_1[Km/W] for single core cables is given by: [12]

$$T_1 = \frac{\rho_T}{2 \times \pi} \times \ln\left[1 + \frac{2 \times t_1}{d_c}\right] \qquad (4.3)$$

ρ_T thermal resistivity of the insulation [Km/W]

d_c diameter of the conductor [mm]

t_1 thickness of the insulation between conductor and screen [mm]

4.2 *Thermal Resistance of Outer Insulation T_3*

The thermal resistance of the outer insulation T_3[Km/W] is given by: [12]

$$T_3 = \frac{1}{2 \times \pi} \times \rho_T \times \ln\left[1 + \frac{2 \times t_3}{D_a'}\right] \qquad (4.4)$$

t_3 is the thickness of outer insulation [mm]

D'_a is the external diameter of the armour (screen) [mm]

4.3 *Soil Thermal Resistance T_4*

The soil thermal resistivity plays a major roll in determining the optimal current ratings and at the same time avoiding overheating and subsequent damaging of underground power cables. The thermal resistivity is a parameter of the soil, which shows how well the soil can dissipate heat away from the heat source. This strongly depends on the water content and vapour movement. For thermally stable soils and for current ratings which avoid drying out of the soil, the thermal resistivity does not change much when heat is applied. This is because, in spite of the fact that water evaporates in the region close to the warm cable and condenses in the cooler regions away from it, sufficient liquid will return due to capillary action, maintaining fairly constant soil moisture level. If the moisture content drops below a certain level, the water return flow through the capillaries is not possible causing the soil surrounding the heat source to dry out. The soil thermal resistivity rises with the sinking of its water content. The soil thermal resistivity depends on its density, texture, mineral composition, temperature and also its moisture content and ability to retain fluids. Artificially made thermally stable materials can be used as backfill in order to control the thermal resistivity around the cable to some extent. [1]

For calculating the permissible current ratings of underground power cables, a partial drying out of the soil must be taken into consideration (see Figure 4.2). For finite element analysis, simulation, the soil is represented as consisting of two regions. The dry region is represented with an eccentric projection of the limit isotherm surrounding the cable with thermal conductivity of 0.4W/Km (dry), and the soil region outside the limit isotherm has a thermal conductivity of 1W/Km (moist). The diameter of the isotherm depends on many variables: depth, cable radius, cable formation, operation mode, conductor power losses, soil properties and ambient temperature.

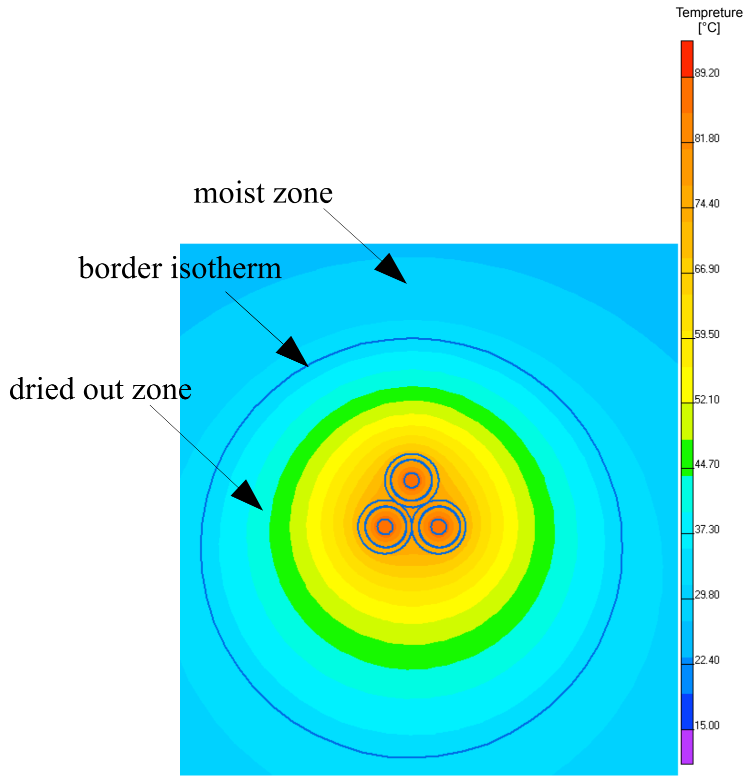

Figure 4.2: Temperature distribution at a maximum continuous load for trefoil formation

The thermal resistivity between the cable surface and the soil surface is denoted with T_4 and for cable in trefoil touching formation and cable in flat formation with equal distance between the phases and equal current load is given in IEC publication 60 287 in the formulas below:

4.3.1 Cable in flat formation with equal distance between the phases and equal losses:[12]

$$T_4 = \frac{1}{2\pi} \times \rho_T \times \ln\left[u + \sqrt{u^2 - 1}\right] + \ln\left[1 + \left(\frac{2 \times l}{s_1}\right)\right] \qquad (4.5)$$

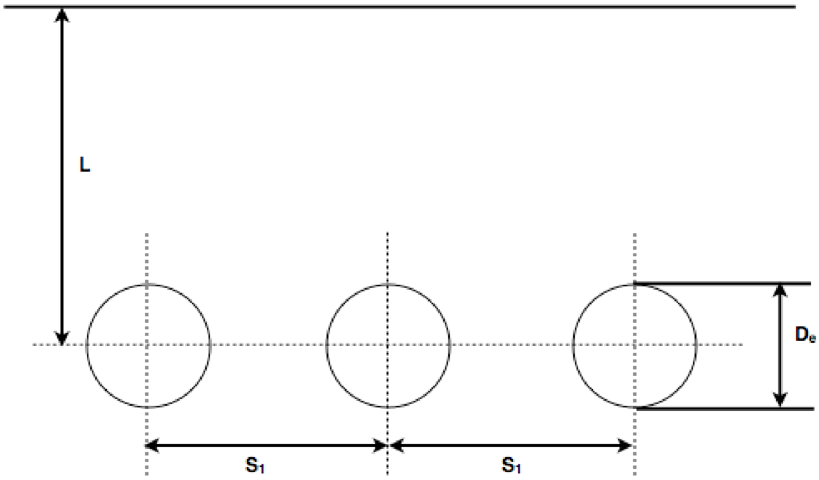

Figure 4.3: Flat formation with equal phase distances

$$u = \frac{2 \times L}{D_e} \quad (4.6)$$

L distance from the surface of the ground to the cable axis [mm]

ρ_T thermal resistivity of the soil [Km/W]

D_e external diameter of one cable [mm]

s_1 axial separation between two adjacent cables [mm]

Here T_4 [Km/W] is given for the middle conductor.

4.3.2 Cable in trefoil touching formation with equal losses:[12]

$$T_4 = \frac{1}{2 \times \pi} \times \rho_T \times [\ln[2u] + 2\ln[u]] \quad (4.7)$$

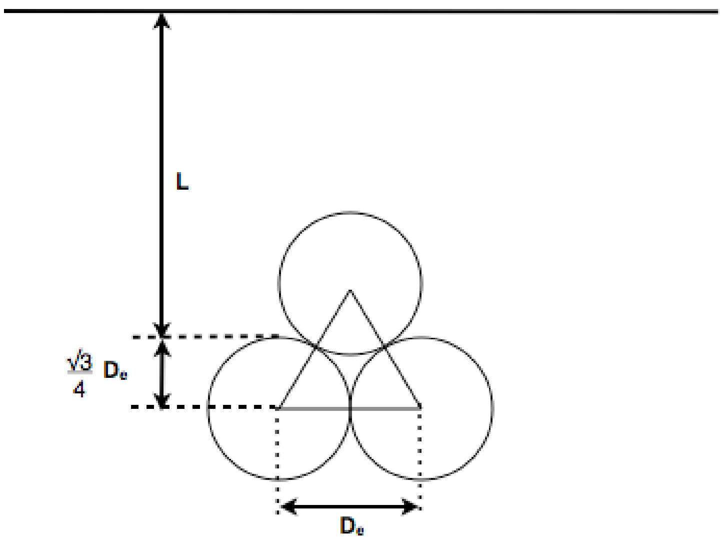

Figure 4.4: Trefoil formation

5 Calculation of Underground Cable Carrying Capacity

5.1 *General*

The current carrying capacity of underground power cables depends on the physical and electrical properties of the cable compounds, the cable length, soil properties and ambient temperature, as described in the previous chapters. In summary the cable ampacity parameters are:

- Conductor material, conductor cross-section and conductor type
- Insulation thickness and insulation dielectric properties
- Cable formation (flat or trefoil), the axial separation between two adjacent cables, depth
- Soil thermal properties

In general the maximum operating temperature rating of the insulation determines the cable ampacity. For XLPE insulation it is 90^0C. [1]

The calculation of the permissible current ratings has the aim of efficiently utilising the cable to its limits, and at the same time preventing damage to and deterioration of the cable.

5.2 *Calculating Permissible Currents Ratings for Buried Cables Using IEC 60 287*

When a permissible current rating is being calculated under conditions of partial drying out of the soil, it is also necessary to calculate a rating for conditions where drying out of the soil does not occur. The lower of the two ratings should be used. [11]

5.2.1 *Buried AC cables where drying out of the soil does not occur*

The permissible current rating of an AC cable can be derived from the expression for the temperature rise above ambient temperature [11]:

$$\Delta\Theta=\left(I^2\times R+\frac{1}{2}\times W_d\right)\times T_1+\left[I^2\times R\left(1+\lambda_1\right)+W_d\right]\times n\times T_2+\left[I^2\times R\times\left(1+\lambda_1+\lambda_2\right)+W_d\right]\times n\times\left(T_3+T_4\right) \quad (5.1)$$

I	current flowing in one conductor [A]
$\Delta\Theta$	conductor temperature rise above the ambient temperature [K]
R	alternating current resistance per unit length of the conductor at maximum operating temperature [Ω/m]
W_d	dielectric loss per unit length for the conductor insulation [W/m]
T_1	thermal resistance per unit length between one conductor and armour [Km/W]
T_2	thermal resistance per unit length of the bedding between sheath and armour [Km/W]
T_3	thermal resistance per unit length of the external serving of the cable [Km/W]
T_4	thermal resistance per unit length between the cable surface and the surrounding medium [Km/W]
n	number of load-carrying conductors in the cable (conductors of equal size and carrying the same load)
λ_1	ratio of losses in the metal sheath to total losses in all conductors in that cable
λ_2	ratio of losses in the armouring to total losses in all conductors in that cable

The permissible current rating is obtained from the above formula as follows [11]:

$$I=\left[\frac{\Delta\Theta-W_d\times[0,5\times T_1+n\times(T_2+T_3+T_4)]}{R\times T_1+n\times R\times(1+\lambda_1)\times T_2+n\times R\times(1+\lambda_1+\lambda_2)\times(T_3+T_4)}\right]^{0,5} \qquad (5.2)$$

5.2.2 *Buried AC cables where partial drying out of the soil occurs*

For single isolated cable or circuit laid at conventional depths, a method based on simple two-zone approximate physical model of the soil should be applied. The zone adjacent to the cable is dried out and the other zone retains the site's thermal resistivity, the zone boundary being an isotherm. This method is considered to be appropriate for those applications in which soil behaviour is considered in simple terms only.

$$I=\left[\frac{\Delta\Theta-W_d\times[0.5\times T_1+n\times(T_2+T_3+\nu T_4)+(\nu-1)\times\Delta\Theta_x]}{R\times[T_1+n\times(1+\lambda_1)\times T_2+n\times(1+\lambda_1+\lambda_2)\times(T_3+\nu\times T_4)]}\right]^{0,5} \qquad (5.3)$$

ν ratio of the thermal resistivities of dry and moist soil ($\nu=\rho_d/\rho_w$)

ρ_d thermal resistivity of the dry soil [Km/W]

ρ_w thermal resistivity of the moist soil [Km/W]

$\Delta\theta_x$ critical temperature rise of the soil. i.e. the temperature rise of the boundary between the dry and the moist zones above the ambient temperature of the soil (θ_x-θ_a) [K]

θ_x critical temperature of the soil and the temperature of the boundary between dry and moist zones [ºC]

θ_a ambient temperature [ºC]

NOTE- T_4 is calculated using the thermal resistivity of the moist soil (ρ_w)

θ_x and ρ_d should be determined from knowledge of the soil conditions. [11]

5.2.3 *Buried AC cables where the drying out of the soil is to be avoided*

Where moisture migration is to be avoided by limiting the temperature rise of the cable surface to not more than $\Delta\theta_x$, the corresponding rating should be obtained from:

$$I=\left[\frac{\Delta\theta_x-n\times W_d\times T_4}{n\times R\times T_4\times(1+\lambda_1+\lambda_2)}\right]^{0,5} \qquad (5.4)$$

However, depending on $\Delta\theta_x$, this may result in a conductor temperature which exceeds the maximum permissible value. The current rating used should be the lower of the two values obtained, either from the above equation or from 5.2.

The conductor resistance R should be calculated for the appropriate conductor temperature, which may be less than the maximum permitted value. An estimate of the operating temperature should be made and, if necessary, subsequently amended. [11]

6 Biological Effects of Alternating Magnetic Fields

6.1 *General*

The effects of electromagnetic fields on biological systems can be very diverse. In general these effects depend on the field intensity and frequency, and also on other factors like body shape and size and also the position of the body in the field. Electric fields can be very easily shielded, but magnetic fields go through most objects like through air.

For low frequency fields, which is the scope of this paper, the stimulation of nerve, sensory and muscle cells is the main impact. The currents induced in the body through the alternating magnetic field are the reason of this stimulation.

6.2 *Impact Mechanisms of Magnetic Fields on the Human Body.*

The impact mechanisms in general are: generation of currents inside the body, deflection of moving electrical charges, resonance (chemical changes), change of the spin orientation in ferromagnetic molecules.

6.2.1 *Eddy currents*

The most important mechanism is the alternating nature of the magnetic fields generated by AC cable systems. This leads to occurrence of electric currents (Faraday law of induction) inside the body. They appear in closed curves around the magnetic filed lines and are referred to as eddy currents.

The following things usually increase the size and effects of eddy currents:

I. The higher the frequency, the more eddy currents

II. The more magnetic field lines are enclosed by the current curves, the bigger the surface area of enclosure the higher are the currents; this means that the current density increases from the centre towards the surface of the body

III. The bigger the body cross section which is exposed to the magnetic field, the higher the eddy currents – the worst case is when the magnetic field lines run perpendicular to the body as the current density in the worst case is almost twice as high as in comparison to the best case when the magnetic filed lines are parallel to our body (see Figure 6.1). [13]

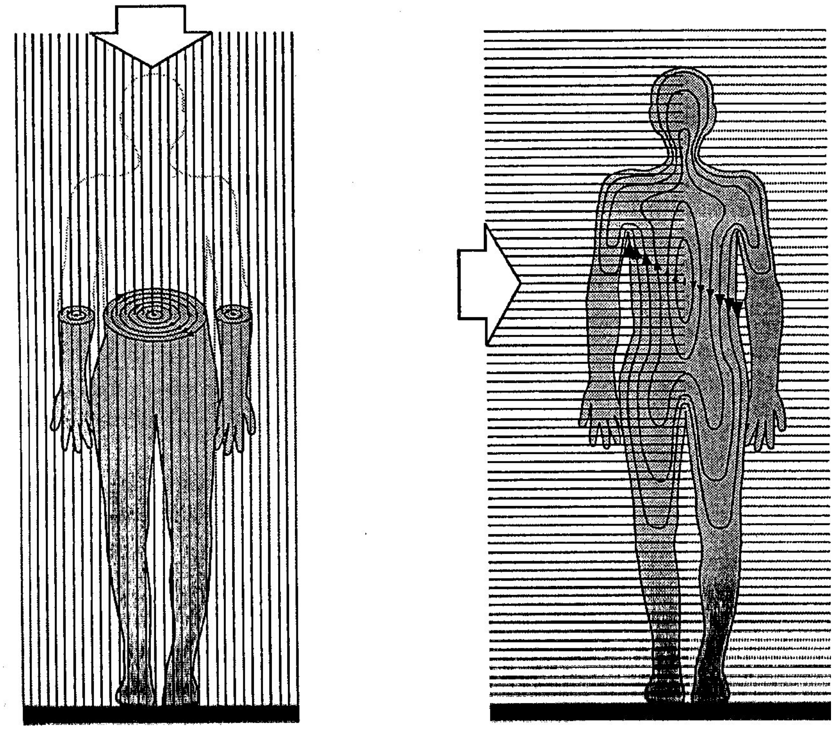

Figure 6.1: Eddy currents induced by alternating magnetic field in the human body [13]

6.2.2 *Deflection of moving electrical charges [Lorenz force]*

The magnetic field can have impact on charges in our body when the charges are moving. The movement of the charges can be because of body functions or because we move in a magnetic field.

When electrical charges are moving through a magnetic field, they can be deflected in different directions (Lorenz force) depending on their charge, thus causing separation between the charges in the body which creates an electrical voltage (electric current density) lateral to the direction of the movement. The voltage increases with the velocity. Such effects can be observed for example in the heart where the fastest movements take place (180m/h), or in the aorta where the velocity of the blood charges can reach up to 25km/h. This mechanism does not depend on the exposed cross-section. [13]

6.2.3 *Resonance (hypothesis)*

Theoretically the varying magnetic field together with the earth magnetic field can induce resonance effects (mesomerism) in the body's molecules. For this to occur, several conditions must be maintained precisely over time, for example there is the frequency and the amplitude of the alternating magnetic field, even the direction of the Earth's magnetic field relative to the alternating magnetic field. These mechanisms are based on hypotheses. They were drawn in order to explain contradictory laboratory results, e.g the change in calcium concentration in isolated chicken brain tissue. This has not been proven experimentally in living body tissue. [13]

The following effects could theoretically occur: [13]

- The bounding force of an electron on the atomic nucleus could change, leading to a change of the probability for a chemical reaction.
- The orientation of the spins of the electrons which participate in a chemical bonding could change, causing change in the probability of chemical bonding.
- The shape of the structure of the molecule could change; in some chemical reactions where two partners bind with the key-lock principle, this could influence the bonding probability.

6.3 *Acute Impacts*

The biological impacts of low frequency magnetic fields can be classified into the following categories

- Stimulation of nerve and muscle cells
- Resonance
- Impacts through long term exposure to low frequency magnetic fields

6.3.1 *Stimulation of nerve and muscle cells*

The most important proven biological impact of alternating magnetic fields is the induction of eddy currents inside the body. These currents can stimulate nerve and muscle cells if three conditions are fulfilled:

I. The current density must have a minimum value of the stimulation signal threshold. The stimulation signal threshold is different for different cells. For the most susceptible nerve cells it is 1µA/cm^2. The muscle cells of the heart are 100 times less susceptible. When the electrical signal is beneath the threshold, the cell does not react (all or nothing rule).

II. The current density must change fast enough in order to stimulate the cells. For frequencies under 50Hz the body cells become less and less susceptible. This is why DC fields cannot stimulate our cells.

III. The impacts have to have sufficient duration in order to stimulate the cells. For frequencies above 100Hz the body cells become less and less susceptible. Above 30kHz up to 100kHz the cells can no longer be stimulated.

In order to research the effects of the eddy currents induced by alternating magnetic fields in the human body, it is necessary first to establish the critical body areas. Since the current density increases towards the surface of the body, the first effects are expected to be noticed at the body surface.

In 1896 the French physicist Jacques-Arsène d'Arsonval described a new phenomena called magnetophosphenes. Magnetophosphenes are flashes of light that are seen when one is subjected to a strong alternating magnetic field. The alternating field causes eddy currents which stimulate the sensitive optical nerves in the retina.

The first glimmer impressions occur in 5% of individuals at frequencies between 20Hz and 30Hz above 2,000µT.

Another critical area of body cells, which are close to the body surface, are the gray nerve cells in the cerebral cortex which we use for all cognitive processes. Nevertheless nerve impulses have a high speed of approximately 430km/h and the charge carriers move relatively slow. A direct influence on these charges, even by the highest generated magnetic fields, is insignificant.

Tests on volunteers have shown no EEG (electroencephalogram) changes caused by 60,000µT (50Hz) magnetic fields. Nevertheless it has been revealed that for such high magnetic fields the shape of the brain signals changes, which was measured at the optical centre. Also there was considerable induction of magnetophosphenes. Permanent changes were not found. After termination of the magnetic field, the initial state of the brain signals returned after some regeneration time.

The pectoral and abdominal muscles are also located very close to the body surface. They are thus exposed to higher current densities than the heart. That is why respiration problems are to be expected prior to ventricular fibrillation. We develop respiration problems because our pectoral muscles start to cramp. This is proven in animal trials: twitching of the pectoral muscles was observed in dogs exposed to very high magnetic fields of 2,500.00μT (50Hz). Heart beat changes were observed in even higher magnetic fields. [13]

6.3.2 *Resonances (mesomerism)*

Already in 1979 it was reported that with exposure to a magnetic field on an isolated chicken brain tissue, the concentration of calcium ions in the culture medium increased. Since then this effect was researched by many groups without reaching a clear outcome: it has been shown that the concentration of calcium ions increases, decreases or stays the same. The probable causes for these effects were assumed to be the change of the probability for chemical bonding or the permeability of the cell membrane for calcium ions. It has been shown that this effect depends on the orientation of the Earth's magnetic field to the alternating magnetic field, but even then some groups have found that the concentration of the calcium ions increases when the earth magnetic field is parallel to the alternating magnetic field, and other groups have found the same effect when the fields are perpendicular to each other. The frequency and the amplitude of the alternating magnetic field also play a role. This effect has disappeared, when the alternating magnetic field was increased. The mechanisms responsible for this effect are still unclear. [13]

6.4 *Limits for Alternating Magnetic Fields*

Establishing the limits for low frequencies magnetic fields is done in two steps:

1. First the basis limits for the current intra-corporeal density are defined. The lowest known threshold (1mA/m^2) is used. The basis limits are then chosen in such a way that a stimulation of nerve and muscle cells can be ruled out. This lies under the lowest threshold with a safety factor. This factor is chosen randomly and is different for different countries. It is between 5 (Germany) and 10 (Austria).
2. It is not possible to prove if the basis limits are not exceeded. Who would allow such a sensor in their body? In the second step, the amplitude of the magnetic field is estimated which will cause that current density inside the body in the worst case (when the magnetic field lines run perpendicular to the body). This is done with mathematical models and the

end results can vary for different countries since different mathematical models are used. In Table 6.1 the prescriptive limits for 50Hz alternating magnetic fields for different countries and organisations are given. [13]

Table 6.1: Prescriptive limits for 50 Hz alternating magnetic fields [13]

County Organization	General population [µT]	Occupationally exposed persons [µT]	Publication
Austria	100	500	ÖN(V)S1119
Germany	424	1 360	Din VDE(V) 0848-4
EU	100	400	Council Recommendation 99/519/EC
Switzerland	100	500	BUWAL 1998
ICNIRP (WHO)	100	500	Health Phys. 1998

Numerous epidemiological studies were done on the risk of different types of cancer, especially childhood leukaemia and the exposure to magnetic fields induced by high voltage transmission lines. The results are very controversial. Nevertheless some countries have established very strict limits which can be under 1µT. These regulations usually apply to new installations near schools, kindergartens, hospitals, etc.

Since the effects of magnetic fields are still unclear, the best thing to do is to keep them as low as possible.

7 QuickField Introduction

QuickField is a finite element analysis system for electromagnetic, thermal and stress design simulation with coupled multifield analysis.

Standard analysis types include: [14]

- Electrostatics
- DC and AC conduction analysis
- Linear and nonlinear transient magnetics
- AC magnetics (involving eddy currents)
- Linear and nonlinear, steady state and transient heat transfer and diffusion
- Linear stress analysis
- Coupled problems

This chapter gives a brief summary of only the models used for this thesis. For a more detailed description, please refer to the QuickField manual which is also available online.

7.1 *What is FEA?*

The aim is to solve the Maxwell equations in a finite number of points. The area where the magnetic field exist is divided into small elements. The field area is covered with a mesh and then the values for the magnetic flux density B and for the magnetic field intensity H are determined for a finite number of points, from which the magnetic flux can be further derived as well as electromagnetic induction, energies, forces and torque. The finite element analysis uses triangles as small areas; in the middle of each triangle the field quantities are solved. It is important to chose the boundaries carefully because almost all programs use boundary conditions which assume that the field there does not exist. If the boundaries are laid too close to the magnetic field but there are actually some insignificant values, this could lead to an error of 10% or more. It is also important to chose a finer mesh in areas where the field changes most rapidly and also in places where the field values are of interest for the application. In areas where low fields are expected, a courser mesh can be used. The mesh is usually automatically generated by the program. [15]

7.2 *Problem Description*

This chapter describes the QuickField models used for the calculation of high voltage underground cables, specifically the permissible currents ratings for buried cables at different laying depths, transient thermal problems for loads above the permissible current ratings, magnetic fields above underground cables, etc.

7.2.1 *AC Magnetic Analysis*

- *Description:*

AC magnetic analysis is used to analyse magnetic fields caused by alternating currents and, likewise, electric currents induced by alternating magnetic fields (eddy currents). The quantities of interest in harmonic magnetic analysis are electric current (and its source and induced components), voltage, generated Joule heat, magnetic flux density, field intensity, forces, torque, impedance and inductance.

Material properties: air, orthotropic materials with constant permeability, current carrying conductors with known current or voltage

Loading sources: voltage, total current, current density, uniform external field

Boundary conditions: prescribed potential values (Dirichlet conditions), prescribed values for tangential flux density (Neumann condition), constant potential constraint for zero flux conditions on the surface of superconductors

Post processing results: magnetic potential, current density, voltage, flux density, field intensity, forces, torque, Joule heat, magnetic energy, impedance, self and mutual inductance

Post processing results: magnetic potential, current density, voltage, flux density, field intensity, forces, torque, Joule heat, magnetic energy, impedance, self and mutual inductance

Special features: A post processing calculator is available for evaluating user-defined integrals on given curves and surfaces. The magnetic forces can be imported into stress analysis on any existing part (magneto-structural coupling); and power losses can be used as a heat source for thermal analysis (magneto-thermal coupling). Two assistance wizards are available for calculation of the mutual and self inductance of coils and for calculation of the impedance. [14]

- *Editing data in AC magnetics*

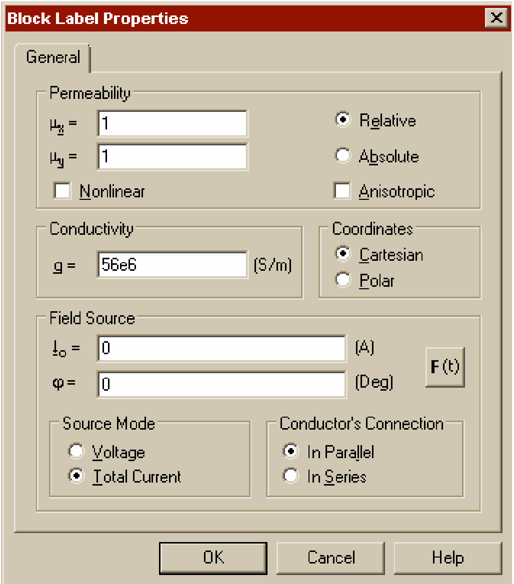

Figure 7.1: Block labels in AC magnetics problem [14]

Block labels in AC magnetics problems can be associated with data containing the values of two components of magnetic permeability tensor, the value of electric conductivity and one of three values defining the field source: source current density, voltage, or total current (see Figure 7.1). When data are associated with a new label, the text boxes for magnetic permeability contain None. Absence of the values in the box for magnetic permeability means that the block with this label will be excluded from the calculations. Thereby to include the blocks in the calculation, the required value of magnetic permeability must be typed in.

As long as Anisotropic is unchecked, QuickField changes the components of magnetic permeability tensor synchronously.

The methods for defining field sources are different for conductors and non-conductive blocks. For solid conductors, either applied voltage or total current is specified. For non-conductive blocks and stranded conductors, a zero conductivity value is specified. In this case QuickField cannot calculate the Joule heat losses of the stranded conductor if the conductivity value is zero. [14]

There are several ways to simulate stranded conductors with QuickField:

1. By drawing each tiny wire in the conductor under the same block label for each conductor,

connected in series

Serially connected conductors always carry the same current. This means that if each tiny wire carries a current of 10A for example, and the whole conductor is composed of 100 tiny wires, the whole current through the conductor will be 1000A. This can be a very time consuming process. That's why cables under $800mm^2$ can be simulated as solid in QuickField since the power losses will only be a few percent higher than for the stranded conductors.

2. By drawing the conductor as a solid one and considering eddy currents to be zero (conductivity is set to zero). In this case Joule heat losses are calculated manually from the manufacturer AC resistivity values with the following formula:

$$P_L = I^2 \times R_{AC} \tag{7.1}$$

P_L	power losses in the conductor [W/m]
R_{AC}	conductor AC resistance at 90^0C [Ω/m]
I	RMS of the applied current [A]

3. By drawing the conductor as being solid and giving a higher conductivity value than the one given by the manufacturer. In this case the conductivity value can be adjusted so that the power losses are the same as those calculated with the above formula.

The cable screen can also make a very important contribution to power losses if it is not cross bounded. Cross bonded screens have a zero conductivity, and screens that are not cross bonded have the conductivity of the material they are made of. The screen can be simulated as a single block if wires are not insulated.

With time-harmonic problems, peak values are always specified for all alternating quantities. [14]

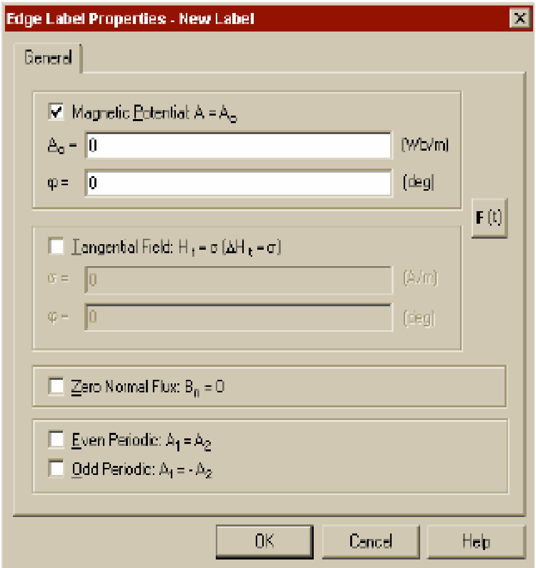

Figure 7.2: Edge labels in AC magnetics problem [14]

Edge labels can be associated with boundary conditions (see Figure 7.2) – select the condition type and enter the appropriate values.

Dirichlet (known magnetic potential) and Neumann (a density of surface current) boundary conditions can depend on position. [14]

7.2.1 *AC Conduction Analysis*

- Description

AC conduction analysis is used to analyse electric fields caused by alternating currents and voltages in imperfect dielectric media. This kind of analysis is mostly used with complex insulator systems and capacitors. Generally the quantities of interest are dielectric losses, voltage, electric filed components, forces and torque.

Material properties: air, orthotropic materials with constant electric conductivity and permittivity

Boundary conditions: prescribed voltage values (Dirichlet condition), prescribed values for boundary current density (Neumann condition), constant potential constraints for describing conductors in surrounding dielectric media

Post processing results: voltage, electric field, current density, power and losses, forces and torque

A post processing calculator is available for evaluating user-defined integrals on given curves and surfaces. Electric forces can be imported into stress analysis on any existing part (elector-structural coupling); and electric losses can be used as a heat source for thermal analysis (electro-thermal coupling).

- *Editing data in AC conduction problems*

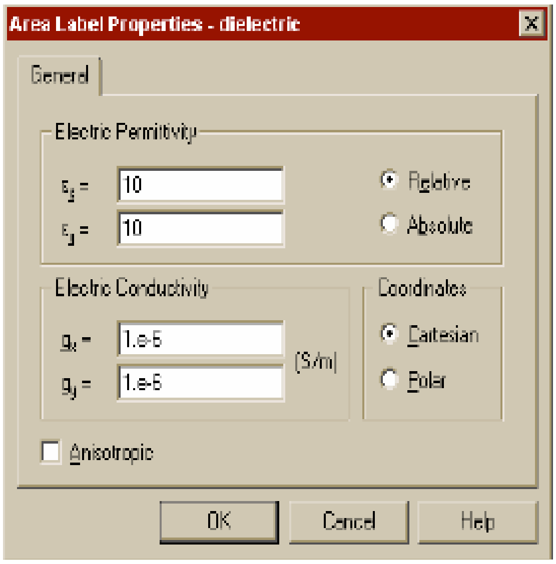

Figure 7.3: Block labels in AC conduction problems [14]

Block labels in AC conduction problems can be associated with data containing the values of two components of electric permittivity tensor and two components of electric conductivity (see Figure 7.3). Blocks with an absence of the values means that blocks with label will be excluded from calculations. To define the material type (thereby including the blocks into calculation) type in the required value of electric permittivity.

As long as Anisotropic is unchecked, QuickField changes the tensor components synchronously. To specify different component values, check Anisotropic before entering the required values. The dialogue labels in addition to tensor components reflect the coordinate system (Cartesian or polar) selected for the property.

With time harmonic problems, you always specify amplitude or peak values for all alternating quantities.

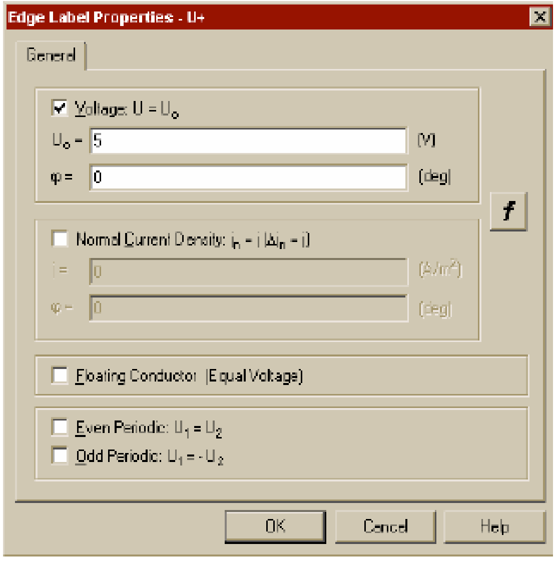

Figure 7.4: Edge labels in AC conduction problems [14]

Edge labels can be associated with boundary conditions. Select condition type and enter appropriate values (see Figure 7.4).

Dirichlet (known voltage) and Neumann (standard component of the current density) boundary conditions can depend on coordinates. A vertex label in AC conduction problem can be associated with known potential or external current values. Check one of the options and enter the appropriate value. [14]

7.2.2 *Thermal Analysis.*

- *Description*

The quantities of interest in thermal analysis are temperature distribution, thermal gradient, and heat losses. Transient analysis allows you to simulate transition of heat distribution between two heating states of a system.

QuickField can perform linear ind nonlinear thermal analysis for 2-D and axisymmetric models. The program is based on heat conduction equation with convection and radiation boundary conditions.

Material properties: orthotropic materials with constant thermal conductivity, isotropic temperature dependent conductivities, temperature dependent specific heat.

Loading sources: constant and temperature dependent volume heat densities, convective and radiative sources, Joule heat sources imported from DC, AC conduction and AC magnetics analysis.

Boundary conditions: prescribed temperatures, boundary heat flows, convection, radiation and prescribed constraints for constant temperature boundaries.

Post processing results: temperatures, thermal gradients, heat flux densities, and total heat losses or gains on a given part; with transient analysis: graphs and tables of time dependency or any quantity in any given point or region.

Special type of inter-problem link is provided to import temperature distribution from another problem as initial state for transient thermal analysis.[14]

- *Editing Data in heat Transfer Problems*

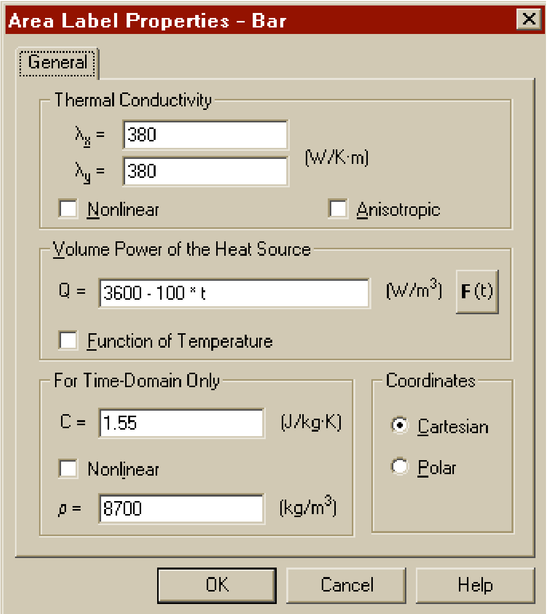

Figure 7.5 Block labels in heat transfer problems [14]

Block labels in heat transfer problem can be associated with data containing two components of thermal conductivity tensor and heat source volume power (see figure 7.5).For transient problems the data should also contain specific heat and volume density values. When you associate data with a new label, the text boxes for thermal conductivity components contain **None**. The word **None** in these boxes or absence of the values means that blocks with the label will be excluded from calculations. To define the material's properties (thereby including the blocks into calculation), type in the required value of thermal conductivity.

As long as **Anisotropic** is unchecked, QuickField changes the components of thermal conductivity tensor synchronously. To specify different components, check **Anisotropic** before entering the required values. The dialog labels besides tensor components reflect the coordinate system

(Cartesian or Polar) selected for the property.

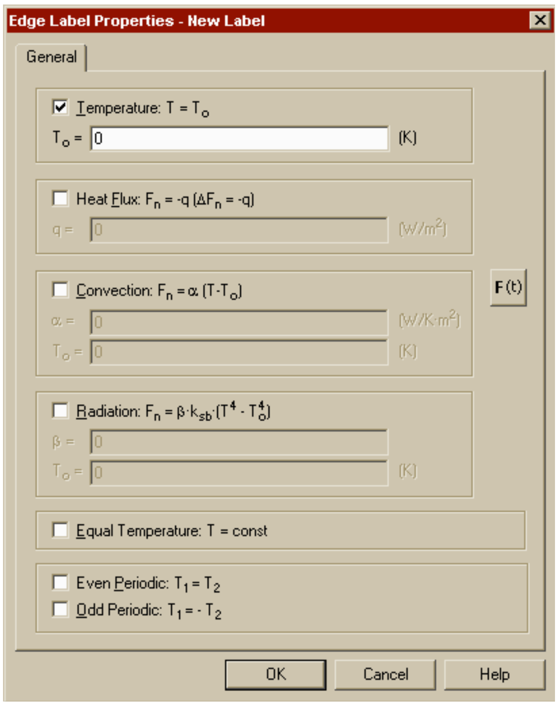

Figure 7.6: Edge labels in heat transfer problems [14]

Edge labels can be associated with boundary conditions. Heat flux, convection, and radiation can be combined together implying that the heat flow through the surface will consist of several components. Check appropriate condition types and enter the required values. Dirichlet (known temperature), Neumann (heat flux), convection and radiation boundary conditions can be coordinate- and, in transient problems, time-dependent (see figure 7.6). To specify coordinate- or time-dependent boundary condition, enter the required formula in place of numerical value.

7.3 *How to Create A Model*

Model development consists of three stages:

- Geometry description
- Definition of properties, field sources and boundary conditions
- Mesh generation

7.3.1 *Creating Model Objects*

In order to create simple geometrical models in QuickField, you define vertices and edges that form boundaries of all subregions having different physical properties. You can use move and duplicate operations to adjust shapes and coordinates of created objects to your needs. To perform editing actions on several objects at once, use the selection tool. Assign labels to blocks, edges and vertices to link them with real world objects such as material properties, boundary conditions and loads. Build mesh in all blocks relevant in field calculation. [14]

For more complex geometrical models, for example Milliken conductors, it is advisable to use a CAD system. You can import model geometry or its fragments from a DXF file produced by any of the popular CAD systems. To do so, click Import DXF in the File menu and enter the required file name in the dialogue. If needed, the window will be automatically zoomed after the import to fit the entire model. [14]

7.3.2 *Meshing Technology*

After creating the geometry of the model or its parts, one can proceed with building the finite element mesh. For highly complex geometry, one can easily build a nonuniform mesh (see Figure 7.7 and 7.8). Fine mesh can be built in some regions (manually) and very coarse in others since the geometric decomposition technique would produce a smooth transition from large to small element sizes. Generally the mesh has to be fine where the field changes most rapidly (high gradient) and also where high precision is needed. In order to save computing time, you can also build a finer mesh by adding artificial vertices in some regions where the field changes most rapidly, leaving the rest with a coarser mesh. [14]

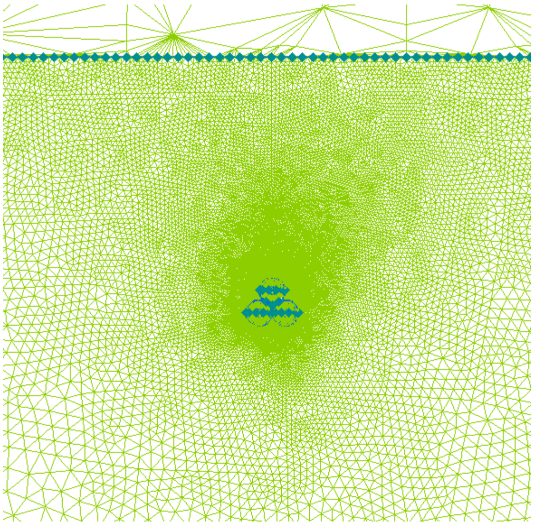

Figure 7.7: Fine mesh automatically generated by QuickField with added artificial vertices in the region of interest

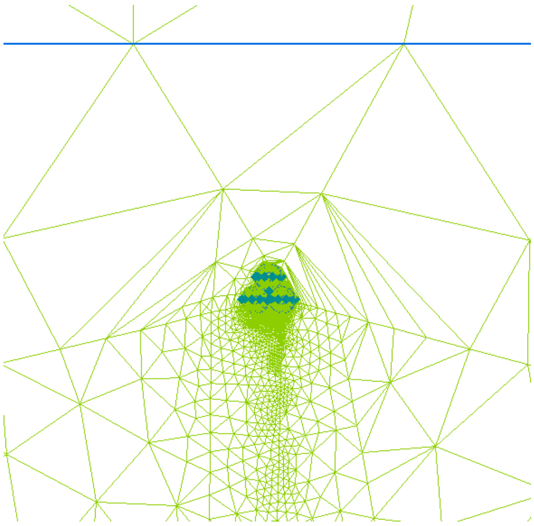

Figure7.8: Coarse mesh automatically generated by QuickField without added artificial vertices

The results obtained by using uniform coarse mesh can significantly differ from the results in which a fine nonuniform mesh is used. In Figure 7.9 below you can see the magnetic field distribution above an underground cable in flat formation simulated with uniform course mesh and then with manually adjusted nonuniform fine mesh, in both simulations the cable has the same current load. The difference between the magnetic fields maxima is approximately 10µT. This is because the field values are calculated in the middle of each triangle (mesh object), so with a higher number of mesh elements the field can be scanned more accurately. This is why it is very important to use the appropriate mesh configuration in order to obtain correct results. This is especially true for estimating magnetic fields above underground cables used in areas where the limits are more strict and the magnetic fields of the cable system are close to these limits. An additional advantage is, in spite of the higher node number of the nonuniform fine mesh, a reduction in simulation time because smaller mesh objects require fewer iterations.

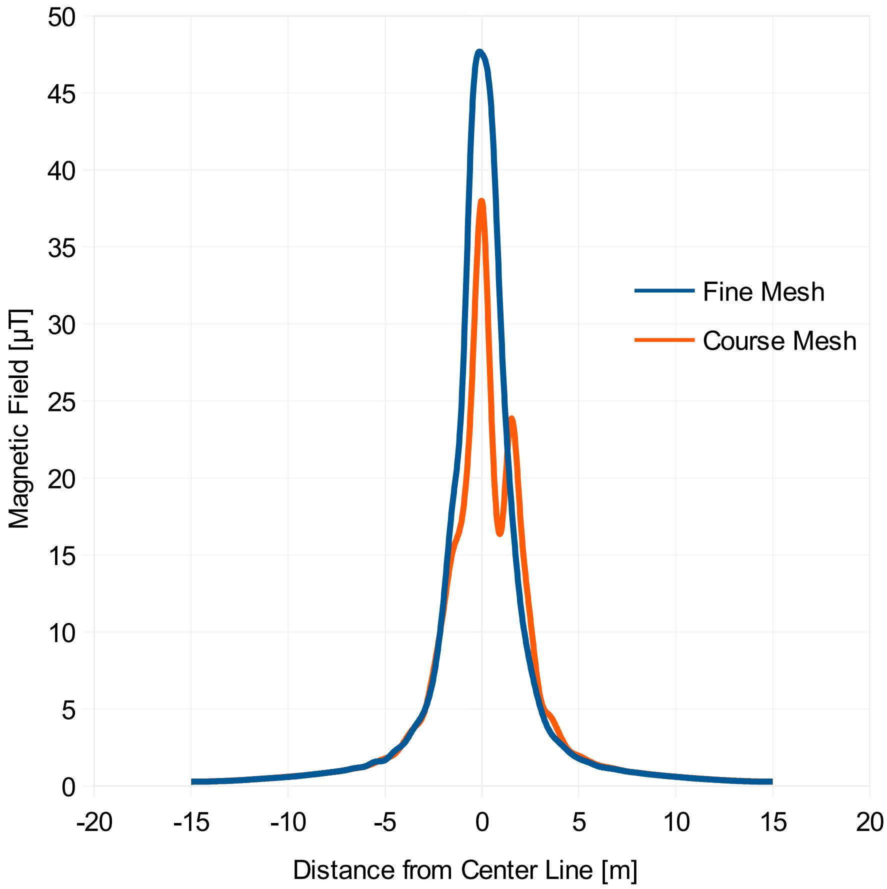

Figure 7.9 Magnetic field above 500kV underground cable buried at 1.2m depth simulated with course mesh and with nonuniform fine mesh.

7.4 *Coupled Problems*

QuickField is capable of importing loads (distributed sources) calculated in some problem into the problem of another type. Following coupling types are supported:

- Heat transfer caused by Joule heat generated in the transient or AC magnetics problem, or DC or AC conduction problem.
- Thermal stresses based on a calculated temperature distribution.
- Stress analysis of the system loaded by magnetic of electric forces.
- A special case of coupling allows for importing of the field distribution in some steady state or transient problem into another transient problem as its initial state. This applies to transient magnetic and transient heat transfer analysis.

In addition to imported loads, you can define any other loads and boundary conditions, similar to non-coupled problem. You can combine several coupling types in one problem. There are several rules to follow with coupled problems:

- Both sources and target problem must share a single model file.
- Both problems must use the same formulation(plane or axisymmetric).
- Sources problem must be up-to -date when solving the target problem.

While importing data from DC or AC conduction problem to heat transfer one, heat sources due to Joule law are assumed in all sub regions included into consideration in both source and target problems. In transient or AC magnetic problems, Joule heat is generated in all conductors. When importing Joule heat from transient magnetic problem into transient heat transfer, both processes are assumed to run synchronously. With this feature, you can simulate time-dependent heat distribution arising from time-dependent electric current distribution (including eddy currents) in a magnetic device. [14]

8 QuickField Implementation

In this chapter several examples were simulated to show how to use QuickField to estimate the thermal impact, magnetic fields, electric and dielectric losses of high voltage underground cables. For the models, a 500kV single core XLPE cable with copper wire screen and with a conductor cross section of $1000mm^2$ will be used from the NKT cables catalogue (see Figures 8.1 and 8.2) with some modifications as described bellow:

- Cable in touching trefoil formation with conductor cross section of $1000mm^2$, simulated as solid and as stranded without any screen, with only one insulation layer
- Cables in flat formation and touching trefoil formation with screens solidly earthed in order to estimate the current and power ratings at a continuous loading of the cables, and conductor and screen losses in different formations
- Cables in touching trefoil and flat formation (1 and 2 circuits) with cross bonded screens in order to estimate the magnetic fields above different formations, current and power ratings, calculating transient problems

500 kV Single Core XLPE Cables with Copper Wire Screen and APL Sheath

Type (A)2XS(FL)2Y 1 x ...... RM/170 290/500 kV with stranded compacted conductor (RM)

Dimensions/Cross Sections			mm²	800	1000
Conductor, Cu or Al, round, stranded, Ø		approx.	mm	34,2	38,1
XLPE insulation		nom.	mm	35,0	33,0
Screen, copper wire, cross section		nom.	mm²	170	170
Outer diameter		approx.	mm	126	126
Cable weight (Cu/Al)		approx.	kg/m	20 / 15	21 / 15
Permissible pulling force (Cu/Al)		max.	kN	40 / 24	50 / 30
Bending radius during laying		min.	m	3,15	3,15
at terminations		min.	m	1,90	1,90
Electrical Data					
Cu conductor DC resistance at 20°C		max.	Ω/km	0,0221	0,0176
Al conductor		max.	Ω/km	0,0367	0,0291
Cu conductor AC resistance at 90°C		approx.	Ω/km	0,0315	0,0265
Al conductor		approx.	Ω/km	0,0492	0,0401
Field strength at U_0 at conductor screen		approx.	kV/mm	14,9	14,8
at core screen		approx.	kV/mm	5,1	5,6
Capacitance per core		approx.	µF/km	0,124	0,137
Inductance		approx.	mH/km	0,45	0,43
Current Ratings/Power Ratings (continuous load)				trefoil installation	
Cu conductor cables	1 circuit		A/MVA	628/544	661/572
	2 circuits		A/MVA	498/431	520/450
Al conductor cables	1 circuit		A/MVA	537/465	577/500
	2 circuits		A/MVA	427/370	455/394

Figure 8.1: NKT cables' data for 500kV single core XLPE cables with copper wire screen and APL sheath [2]

The current ratings are calculated for standard conditions, which are:	
soil thermal resistivity, moist/dry	1,0/2,5 Km/W
soil temperature	15 °C
laying depth	1,2 m
for cables in touching trefoil formation, screens solidly earthed	
axial distance of two circuits	0,5 m
cables in flat formation, screens cross bonded	
axial distance between phases	0,2 m
axial distance of two circuits	0,9 m

Figure8.2: NKT cables' data for soil thermal resistivity, laying depth and axial distance between phases and circuits [2]

8.1 *Power Losses and Power Ratings of Solid and Stranded Conductors*

In this example a cable in touching trefoil formation was simulated both with solid and with stranded conductors having the same surface area. From these simulations one can see the differences in power losses between cables with solid and cables with stranded conductors.

8.1.1 *Geometry of the Models*

Since in this problem only the conductor's power losses are of interest, the screen in both simulation models (solid and stranded conductors) will be omitted and the insulation will be drawn as a single layer. The geometry of the models is similar to the one shown in Figure 8.6.

- Cable in touching trefoil formation with solid conductors

The ground where the cable is buried is simulated as a block with measurements 30m×30m, the air above the ground is simulated as a block with measurements 30m×3m. The cable is 1.2m under the air boundary and about 15m on the right and on the left from the side boundaries of the ground. It is important to take big enough boundaries surrounding the cable in order to obtain correct results.

Table 8.1: Cable geometrical parameters

Conductor cross section	35.7mm
Insulation thickness	50mm

- Cable in touching trefoil formation with stranded conductors

Each conductor consists of 50 wires with 20mm^2 cross section. The insulation thickness around the conductor is 50mm. The ground and the air blocks have the same measurements as in the model with solid conductors.

8.1.2 *Required parameters*

To estimate the power losses in the conductors, an AC magnetics problem is simulated for each cable. For both cases the current peak value is 1000A. The conductor's conductivity g [S/m] is calculated with the following formula:

$$g=\frac{1}{(R_{AC}\times A)} \qquad (8.1)$$

R_{AC} conductor AC resistance at 90ºC [Ω/m]

A surface area of the conductor [m^2]

The following parameters are required:

- Cable with solid conductors

Table 8.2: AC magnetics problem parameters for cable with solid conductors

	Relative permeability	*Conductivity [S/m]*	*Total Current [A] Phase [deg]*
Air	1	0	0
Soil	1	0	0
Conductor (1,2,3)	1	37.7×10^6	1000A [Phase], consider as a single one
Insulation	1	0	0

All edge labels have no values.

- For cable with stranded conductors

Each conductor consists of 50 wires under the same block label. The wires in each conductor are connected in series and carry a current of 20A which means that the conductor's total current will be 1000A (see Table 8.3).

Table 8.3: AC magnetics problem parameters for cable with stranded conductors

	Relative permeability	*Conductivity [S/m]*	*Total Current [A] Phase [deg]*
Air	1	0	0
Soil	1	0	0
Conductor (1,2,3)	1	37.7×10^6	20A [Phase], connected in series
Insulation	1	0	0

All edge labels have no values.

8.1.3 *Results*

After the simulations were finished, an integral is drawn around one of the conductors in each model and the power losses are obtained with QuickField integral calculator under Joule heat as an average value. Table 8.4 shows the power losses per conductor for stranded and solid conductor obtained with QuickField and with formula 8.1.

Table 8.4: Power losses per conductor

	Power losses per conductor [W/m] for peak current value of 1000A
Trefoil formation with stranded conductors (QuickField)	13.25
Trefoil formation with solid conductors (QuickField)	15.6
Trefoil formation (theoretical calculation)	13.25

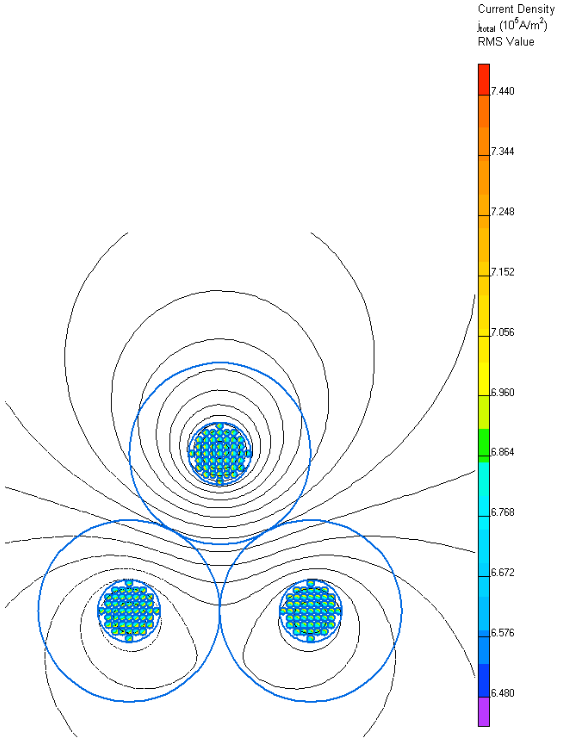

Figure 8.3:Current density distribution in trefoil formation with solid conductors

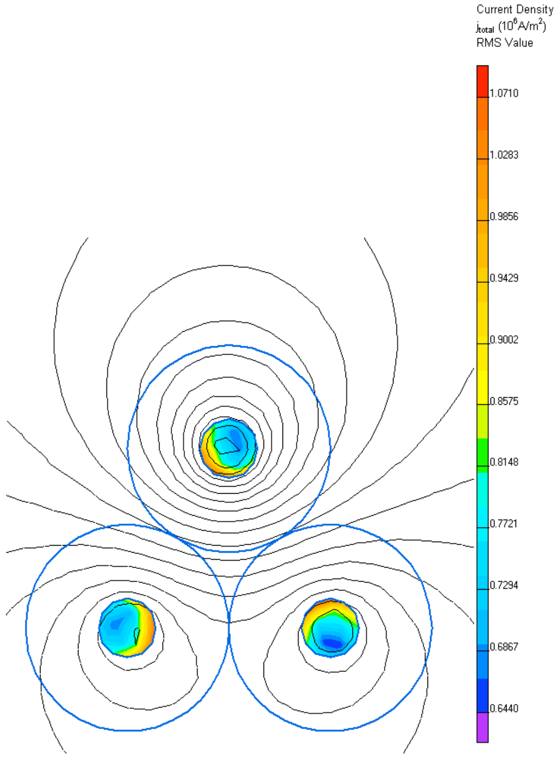

Figure 8.4:Current density distribution in trefoil formation with stranded conductors

From Figure 8.3 and Figure 8.4 above, one can see that the current density in the solid conductors is not evenly distributed throughout their cross-section; this is due to skin and proximity effects. The current density in the stranded conductors is evenly distributed. The skin and proximity effects increase the effective resistance of the conductor leading to higher power losses (Joule heat losses). The power losses in solid conductor are approximately 18% higher (for a conductor surface area of 1000mm^2) than in stranded conductors. This leads to lower power transfer ratings with solid conductors since higher Joule heat losses lead to higher temperatures in the conductors. The power losses for solid conductors with bigger cross sections can be more than 40% higher than for stranded conductors due to skin and proximity effects. This is why the conductors for high voltage underground cables are usually stranded and for conductors with big surface areas they can be also stranded segmented in order to further reduce the Joule heat losses.

8.2 *Power Transfer Ratings for Cables in Different Formations with Solidly Earthed Screens*

This example shows the difference in power transfer ratings and power losses for cables in different formations (trefoil and flat) with screens solidly earthed. The conductors in both formations have the same geometry and the same physical parameters.

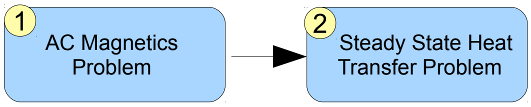

Figure 8.5: Step diagram for estimating the maximum continuous current load

Figure 8.5 shows the simulation path in order to to estimate the power transfer ratings for continuous load. In this case, two QuickField problems for each cable formation will be simulated: an AC magnetics problem in order to estimate the Joule heat losses in the conductors and the screens and a steady state heat transfer problem in order to see the temperature distribution within the cables and the surrounding area. The steady state heat transfer problem is linked to the AC magnetics problem for the corresponding cable formation.

8.2.1 *Geometry and parameters of the model*

The geometric model of 500kV single core XLPE cable with copper wire screen and with stranded conductors with a cross section of 1000mm^2 was built in QuickField according to the catalog data (see Figure 8.1). The conductors are simulated as solid in QuickField, in this case a higher conductivity value will be used in order to obtain the same conductor Joule heat losses, as if the conductors were stranded. This can be done by adjusting the conductivity in QuickField until the desired power loss is reached. The conductor power losses are calculated with formula 8.1:

$$P_L = I^2 \times R_{AC} \quad \text{[W/m]}, \text{ for this example } R_{AC}=0.0265 \text{ [}\Omega\text{/km]}.$$

The screen is designed with a cross section of 170mm^2.

Table 8.5: Cable's geometric parameters.

Conductor's cross section	38.1 mm
Inner insulation thickness	33mm
Screen thickness	0.5mm
Outer insulation thickness	10.5mm

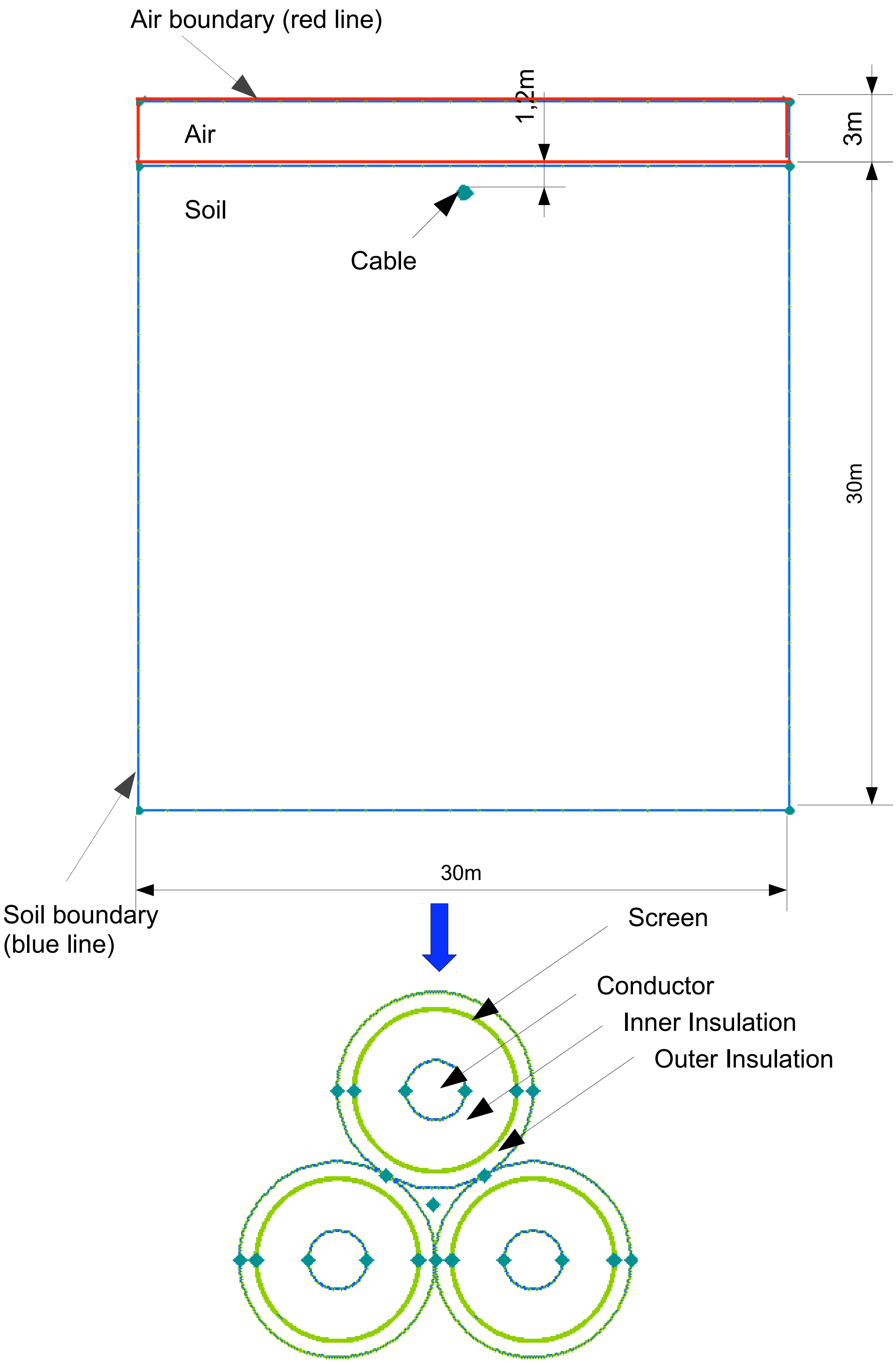

Abbildung 8.6: Geometry of the cable in trefoil formation simulated using QuickField

- Required data for the AC magnetics problem

Block labels

In Table 8.6 the AC magnetics parameters are given for the cable with stranded conductors, simulated as solid conductors with higher conductivity. This is done as it is easier to build the model, and by giving the solid conductor higher conductivity as given by the manufacturer it will have the same power losses as if the conductor was stranded.

Table 8.6: AC magnetics problem block label's parameters

	Relative permeability	*Conductivity [S/m]*	*Total Current [A] Phase [deg]*
Air	1	0	0
Soil	1	0	0
Conductor (1,2,3)	1	39.3×10^{6}	Peak value of the current [Phase], consider as a single one
Screen	1	45×10^{6}	0
Inner insulation	1	0	0
Outer insulation	1	0	0

All edge labels have no values.

- Required data for the steady state heat transfer problem

Block labels

Table 8.7 and Table 8.8 contain the parameters required for the steady state heat transfer problem for cables with stranded conductors, simulated as solid conductors. The volume power of the conductors is zero since it is transferred from the AC magnetics problem. The volume power of the insulation is calculated manually with the formula below:

$$Q_i = \frac{W_d}{A} \tag{8.2}$$

Q_i volume Power of the insulation [W/m^3]

W_d dielectric losses per phase [W/m], calculated with formula 3.11

A insulation surface area [m^2]

The soil thermal conductivity is 1W/Km when the soil is simulated as being uniformly moist. For calculations in which partial drying out of the soil is to be considered, the thermal conductivity is defined as a function of temperature. In order to do this, check Nonlinear in the Thermal Conductivity field group. This will get you into temperature curve editor for defining λ =λ(T). For moist soil, the thermal conductivity is 1W/Km and for dry soil, which occurs near the cable, it is 0.4W/Km (see Figure 8.7). For this simulation the border between the moist and dry soil lies at the 35ºC isotherm; this border depends on the soil properties as mentioned earlier.

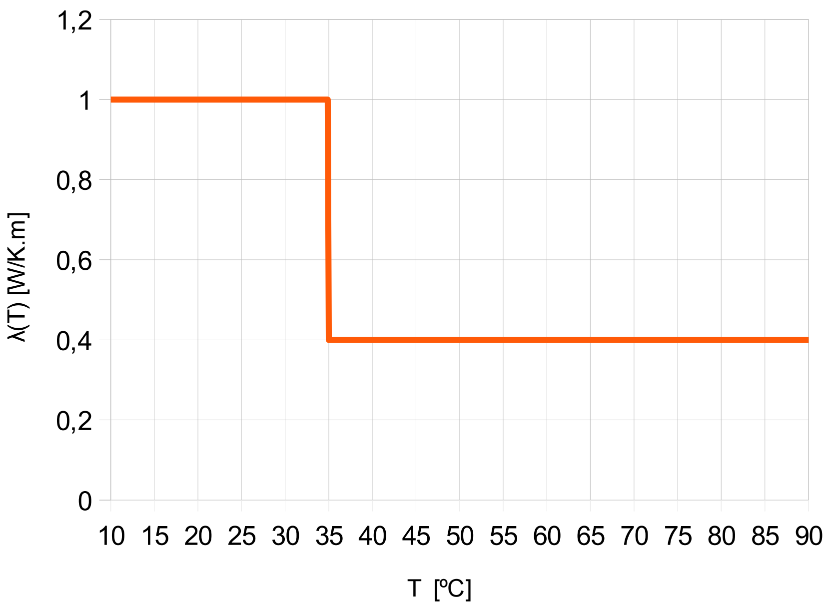

Figure 8.7 Thermal soil conductivity as function of temperature

Table 8.7: Steady state heat transfer problem block label parameters

	Volume Power of the Heat Source [W/m³]	*Thermal Conductivity [W/Km]*
Air	0	0.03
Soil	0	1 or λ(T)
Conductor (Cu) (1,2,3)	0	400
Inner insulation (XLPE)	421	0.28
Outer insulation (PE)	0	0.38
Screen (Cu)	0	400

Table 8.8: Edge label values for steady state heat transfer problem

	Temperature [°C]
Air boundary	15
Soil boundary	15

8.2.2 *Results*

- Power losses

Table 8.9 shows the power losses per conductor and per screen in different formations (trefoil and flat) calculated with QuickField. Power losses for certain block or blocks (conductor or screen) are calculated first by defining the contour of interest in the active field window and then pressing the **Integrals** button. Power losses of the selected contour or contours are represented as Joule heat in the **Integral Calculator** menu which appears on the left side of the active field picture. One can select the block of interest by drawing an integral around it or by using **Pick Elements** option in the drop down menu and **Contour** from the menu bar.

Table 8.9: Power losses

	Power Losses [W/m] for peak current value of 1000A
Conductor in trefoil formation	13.22
Conductor in flat formation	13.22
Screen in trefoil formation	10.7
Screen in flat formation	32.65

- Current ratings / power ratings (continuous load)

In Table 8.10 the current ratings and the power ratings are shown for continuous load for trefoil and flat formation with screens solidly earthed as calculated with QuickField.

Table 8.10: Current ratings/ power ratings

	Current ratings [A]	*Power ratings [MVA]*
Trefoil formation	690	597
Flat formation	628	543

Table 8.11 shows the results obtained with QuickField and with IEC publication standard 60-287 formulas for trefoil formation with screen solidly earthed.

Table 8.11 Current ratings/power ratings for trefoil formation

	Current ratings [A]	*Power ratings [MVA]*
QuickField	690	597
IEC publication 60-287	661	572

8.2.3 *Discussion of results*

Since the screen power losses in flat formation are about three times higher than the losses in trefoil formation, the power transfer ratings for continuous load are lower in flat formation with screen solidly earthed than in trefoil formation. This is why, in order to reduce screen losses, trefoil formation is used or the screens are cross bonded.

Also the results obtained with QuickField are similar to the results calculated with IEC publication 60 287 standard formulas.

8.3 *Cables in Touching Trefoil and Flat Formation(1 and 2 Circuits) with Cross Bonded Screens*

This example shows how to estimate for different formations the magnetic fields, current/power ratings and how to calculate transient overload problems.

The same geometry model was used as described in point 8.2. Since the screens are cross bonded, their electric conductivity value will be set to zero. For two circuits, the axial distance between the circuits is 0.9m for flat formations and 0.5m for trefoil formations as in the NKT cable catalogue (see Figure 8.2).

8.3.1 *Estimating the magnetic field above underground cables with QuickField*

In order to estimate the magnetic field above underground cables, an AC magnetics problem is simulated.

8.3.2 *Required parameters*

In Table 8.12 one can see the required block label values for cable simulated in an AC magnetics problem with stranded conductors, simulated as being solid. The conductor conductivity has a higher value than the one recommended by the manufacturer in order to obtain the same Joule heat losses as if the conductor was stranded. The screen conductivity is set to zero because it is simulated as cross bonded.

Table 8.12: Required block label values for cable simulated in AC magnetics problem

	Relative permeability	*Conductivity [S/m]*	*Total Current [A] Phase [deg]*
Air	1	0	0
Soil	1	0	0
Conductors	1	39.3×10^6	Peak value of the current [Phase], consider as a single one
Screen	1	0 (cross bonded)	0
Inner insulation	1	0	0
Outer insulation	1	0	0

All edge labels have no values.

8.3.3 *Analysing the solution*

After the simulation is finished, the magnetic field values are measured on the ground surface above the underground cables. This can be done by examining local field values-values of physical quantities at the specified points or by integrating over the line or surface defined by the specified contour. A table or a plot that shows the distribution of local field values along the selected contour can be built by clicking on the “table” or “chart” symbol in the upper right corner of the window. [14] In this case the results are shown for equidistant points along the specified line, and one can manually adjust the step length between the result points. It is important to choose a smaller step in order to see all the values, especially in areas where the field changes rapidly.

8.3.4 *Results*

The magnetic field is measured at ground level above the cables. The current load for all systems is set to 1000A (1414A peak value). This value is chosen since it is easier to estimate the magnetic field for different currents by simply multiplying the value of the magnetic field for 1000A by the new current value.

For example the magnetic field for 1500A will be 1.5 times bigger then the magnetic field for 1000A.

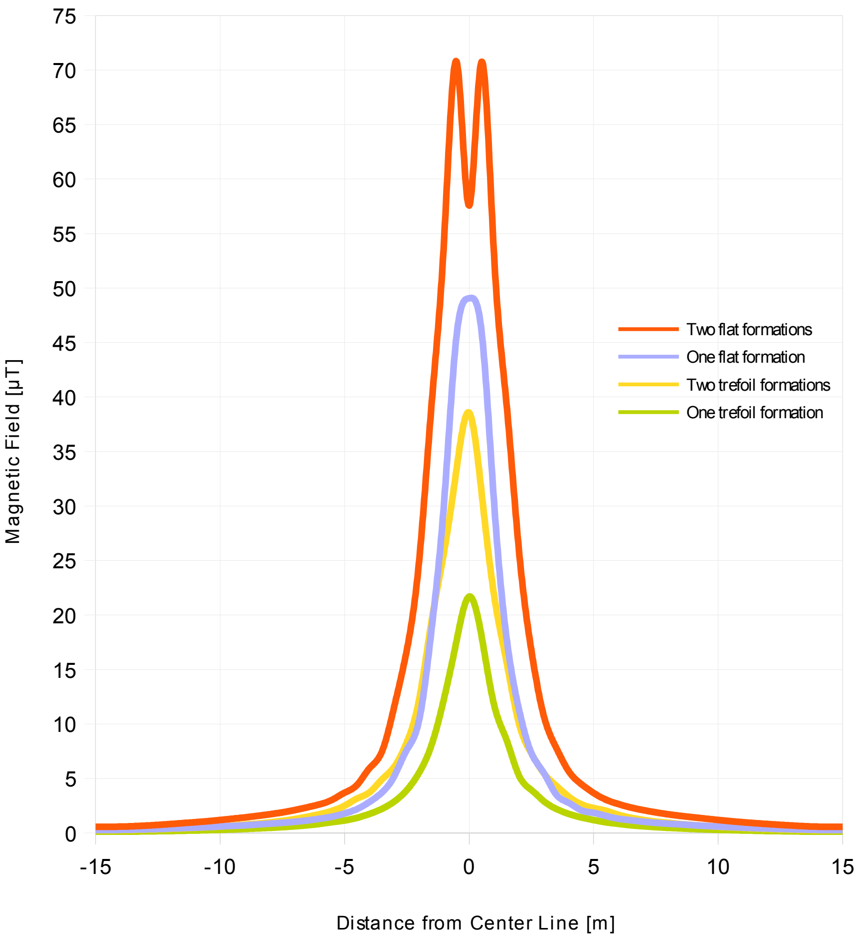

Figure 8.8: Magnetic fields above 500kV underground cables buried at 1.2m depth, loaded with 1000A

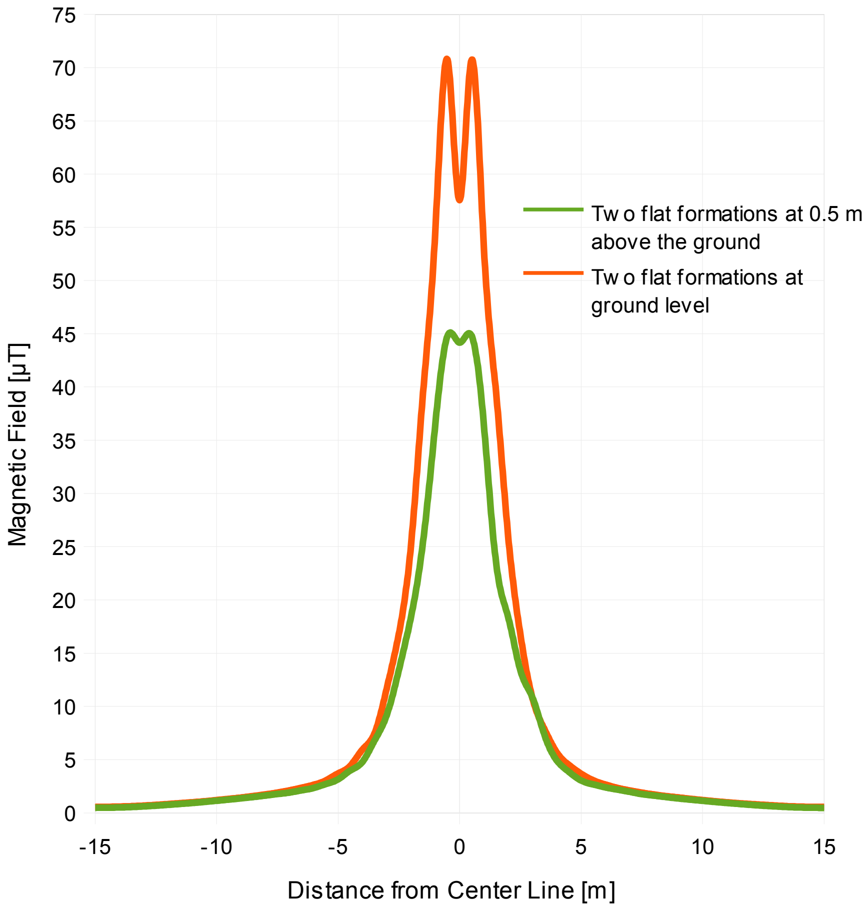

Figure 8.9: Magnetic fields measured at ground level (red) and 0,5m above ground (green) for two flat formations at 1000A load and 1.2m laying depth.

8.3.5 *Discussion of the results.*

From Figure 8.8 one can see that the magnetic fields above the flat formations (single and double) are much higher than above the trefoil formations. This is because the magnetic fields in trefoil formations cancel each other out due to the geometry of the cable.

Magnetic fields from underground cables can be reduced through burying them deeper in the ground (see Figure 8.9) and/or through 'phase' cancellation using a trefoil formation.

The fields are higher close to the cables and rapidly decline with distance. This is why the highest field levels for an underground cable will only be directly above the cable during maximum current flow. In general, magnetic fields from underground cables fall much faster with distance than those from corresponding overhead lines, but they can be actually higher at small distances from the cable since the cables are usually closer to the exposed person than the overhead lines.

8.4 *Estimating the Permissible Currents Ratings for Continuous Load*

Since the maximum temperature of the cable outer insulation (polyethylene sheath) can be 80°C and the conductor maximum temperature can be 90°C at continuous load, the current must be chosen in such a way that these temperatures don't become too high and at the same time the maximum power is transferred. There are several ways to solve this problem, outlined below.

a) Only a steady state heat transfer problem by calculating the volume power of the heat source for the conductors and the insulation using formulas 8.3 and 8.2 and adding these values in the specified block labels.

- Required parameters

Table 8.13: Block label values for steady state heat transfer problem

	Volume Power of the Heat Source [W/m^3]	*Thermal Conductivity [W/Km]*
Air	0	0.03
Soil	0	1 or λ(T)
Conductor (Cu)	Q_c	400
Inner insulation (XLPE)	421	0.28
Outer insulation (PE)	0	0.38
Screen (Cu)	0	400

$$Q_c = \frac{I^2 \times R_{AC}}{A} \qquad (8.3)$$

where

Q_c volume power of the conductor [W/m^3]

I RMS of the current [A]

R_{AC} conductor AC resistance at 90^{0}C [Ω/m]

A conductor's surface area [m^2]

The volume power of the insulation Q_i is calculated with formula 8.2.

- Edge labels

In Table 8.14 the required edge labels values are given for the steady state heat transfer problem. The air boundary and the soil boundary are set first to 15° and then to 20°C in order to show the power ratings at continuous load for different temperatures. The conductor surface and the outer surface of the cable have no values since their temperature will change depending on the surrounding temperature and on the load.

Table 8.14: Edge labels values

	Temperature [°C]
Air boundary	15 or 20
Soil boundary	15 or 20
Outer surface of the cables	none
Conductor's surface	none

b) Steady state heat transfer problem with links to the AC conduction problem and AC magnetics problem (see Figure 8.10); all three problems must have the same geometry file.

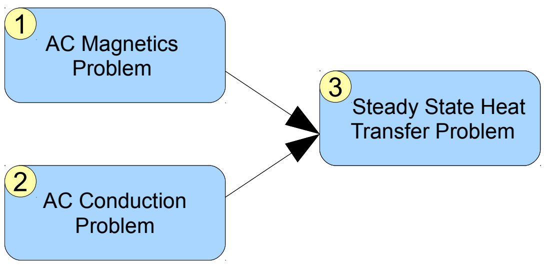

Figure 8.10: Step diagram for estimating the maximum current load at continuous mode

1. An AC magnetics problem in order to calculate the Joule heat generated in the conductors during a continuous load. The current must be adjusted so that the temperature of the outer insulation does not exceed 80°C. The problem is simulated with the same block and edge labels as described in point 8.2.

2. An AC conduction problem to calculate the dielectric losses in the insulation

   The parameters for the cable simulated in AC conduction problem are listed in Table 8.15. For the conductors blocks there are no values; that means they will not be included in the calculation because in this simulation only the dielectric losses are of interest, which depends on the applied voltage. In Table 8.16 the required edge labels are listed. For each conductor surface, the peak value of the voltage per phase and the phase must be added.

3. A steady state heat transfer problem in order to obtain the temperature field of the underground cables at continuous load

   It has two links as generated heat: AC conduction problem and AC magnetics problem.

   In Table 8.17 the block label parameters are listed for cable simulated in a steady state heat transfer problem. The soil is represented with two zones as described in the previous examples. The volume powers of the heat sources are set to zero because these values are transferred from the AC conduction and AC magnetics problem which are linked to the steady state heat transfer problem.

   In Table 8.18 the required edge labels are listed for cable simulated in the steady state heat transfer problem. The air boundary and the soil boundary are first set to 15°C and then to 20°C in order to see the difference in power ratings at different temperatures. The outer surface of the cables and the outer surface of the conductors have no values since they change with the load.

Table 8.15: Block label parameters for AC conduction problem

	Relative electric permittivity	*Electric conductivity [S/m]*
Air	1	0
Soil	2.3	0
Conductor (Cu)	none	none
Inner insulation	2.3	Manufacturer data
Outer insulation	2.3	Manufacturer data
Screen	2	0

Table 8.16: Edge label parameters for AC conduction problem

	Voltage [V], Phase [deg]
Air boundary	0
Soil boundary	0
Outer surface of the cables	0
Conductor's surface	Peak Value per Phase (Phase=0,120,240)

Table 8.17: Block label parameters for steady state heat transfer problem

	Volume Power of the Heat Source [W/m^3]	*Thermal Conductivity [W/Km]*
Air	*0*	0.03
Soil 1	*0*	1 or λ(T)
Conductor 1,2,3 (Cu)	*0*	400
Inner insulation (XLPE)	*0*	0.28
Outer insulation (PE)	*0*	0.38
Screen (Cu)	*0*	400

Table 8.18: Edge label parameters for steady state heat transfer problem

	Temperature [° C]
Air boundary	15 or 20
Soil boundary	15 or 20
Outer surface of the cables	none
Conductor's surface	none

c) Combination of the two methods

In my simulation I used a combination of the two methods since the dielectric losses depend only on the voltage which does not change. I have added the values of the volume power of the insulation directly into the steady state heat transfer problem which has a link only to the AC magnetics problem (see Figure 8.5).

- Required data for the AC magnetics problem are listed in Table 8.19:

Table 8.19: Block label parameters for AC magnetics problem

	Relative permeability	*Conductivity [S/m]*	*Total Current [A]* *Phase [deg]*
Air	1	0	0
Soil	1	0	0
Conductor (1,2,3)	1	39.3×10^6	Peak value of the current [Phase], consider as a single one
Screen	1	0 (cross bonded)	0
Inner insulation	1	0	0
Outer insulation	1	0	0

The edge labels for AC magnetics problem have no values.

- Required data for steady state heat transfer problem

In Table 8.20, the block label values are listed; in this case the inner and the outer insulation have values for the volume power of the heat source which are calculated using the formula for dielectric losses and the formula for the volume power of the heat source. The conductors have no value for the volume power of the heat source since it will be transferred from an AC magnetics problem. Table 8.21 gives the edge labels parameters for steady state heat transfer problem.

The thermal conductivity values are standard and can be found on the internet.

Table 8.20: Block label parameters in steady state heat transfer problem

	Volume Power of the Heat Source [W/m³]	*Thermal Conductivity [W/Km]*
Air	0	0.03
Soil	0	1 or λ(T)
Conductor (Cu) (1,2,3)	0	400
Inner insulation (XLPE)	421	0.28
Outer insulation (PE)	0	0.38
Screen (Cu)	0	400

Table 8.21: Edge label parameters for steady state heat transfer problem

	Temperature [°C]
Air boundary	15 or 20
Soil boundary	15 or 20
Outer surface of the cable	none
Conductor surface	none

8.4.1 *Results*

Below are the results after simulating the problems.

Table 8.22 shows the maximum current ratings/power ratings at continuous load for cable in different formations and different number of circuits calculated with QuickField with partial drying out of the soil and a soil temperature of 15 ºC.

Table 8.22: Maximum current ratings/ power ratings for soil temperature of 15ºC

	Current ratings/power ratings (continuous load) [A/MVA]
Flat installation (one circuit)	955/826
Flat installation (two circuits)	765/660
Trefoil installation (one circuit)	884/765
Trefoil installation (two circuits)	660/560

Table 8.23 shows the maximum current ratings/power ratings at continuous load for cables in trefoil and flat formation for one and two circuits calculated with QuickField with partial drying out of the soil and a soil temperature of 20ºC.

Table 8.23: Maximum current ratings/ power ratings for soil temperature of 20°C

	Current Ratings/Power Ratings (continuous load) [A/MVA]
Flat installation (one circuit)	880/760
Flat installation (two circuits)	720/620
Trefoil installation (one circuit)	840/720
Trefoil installation (two circuits)	615/530

8.4.2 *Discussion of the results*

Higher power can be transferred with a flat formation which has the same parameters as the trefoil formation (only when the screens are cross bonded). This is because the conductors in trefoil formation are in touching configuration, so they are heating each other.

8.4.3 *Comparison of the results obtained with QuickField and IEC 60 287 standard for cable in trefoil formation*

In Table 8.24 one can find the permissible current ratings/power ratings for cable in single trefoil formation with cross bonded screen, calculated with QuickField and the IEC 60 287 standard for partial drying out of the soil and for two different boundary temperatures.

Table 8.24: Maximum current ratings/ power ratings for trefoil formation (one circuit)

Temperature of the soil	*QuickField [A/MVA]*	*IEC 60 287-2-1 [A/MVA]*
15°C	884/760	835/720
20°C	860/740	810/700

The results for permissible currents ratings at continuous load obtained with QuickField are slightly higher than the results calculated with IEC 60 287 standard.

Table 8.25 shows the results for permissible current ratings/power ratings for cable in single trefoil formation with cross-bonded screen and without drying out of the soil, calculated with QuickField and the IEC 60 287 standard.

Table 8.25: Maximum current ratings/ power ratings for trefoil formation (one circuit)

Temperature of the soil	*QuickField* *[A/MVA]*	*IEC 60 287-2-1* *[A/MVA]*
15ºC	1089/942	1089/942
20ºC	1050/905	1050/905

8.5 *Calculating Transient Problems with QuickField.*

In this example, the time in which the hottest conductor will reach 90°C from a 60% continuous load to 150% transient load and the time in which the conductor will cool down to the initial temperature from 90°C with 50% load will be estimated (see Figure 8.11).

8.5.1 *Required data*

For this example several QuickField problems were simulated as shown in Figure 8.10 below. The temperature of the soil is set to 15°C. All problems use the same geometry file. The data are added as described in the previous examples. First an AC magnetics problem 1 was simulated with 60% of the maximum continuous current load. This problem is then linked to a steady state heat transfer problem where the temperature field of the cable system and its surroundings at 60% contentious load is calculated. Then AC magnetics problem 2 with a 150% of the maximum continuous load was simulated. The temperature field from the steady state heat transfer problem 1 was linked to the transient heat transfer problem 1 and the AC magnetics problem 2 was also linked to this transient heat transfer problem as generated heat. The transient heat transfer problem is simulated for 24 hours with 1h steps. After the simulation, the temperature field of the cable system and its surrounding area is obtained for each hour. By looking through the results, it is easy to find out when the hottest conductor will reach 90°C. Then the temperature field of the simulation at the time in which the hottest conductor reaches 90°C was linked to transient heat transfer problem 2, along with an AC magnetics problem 3 loaded with 50% of the maximum continuous load for the cable formation.

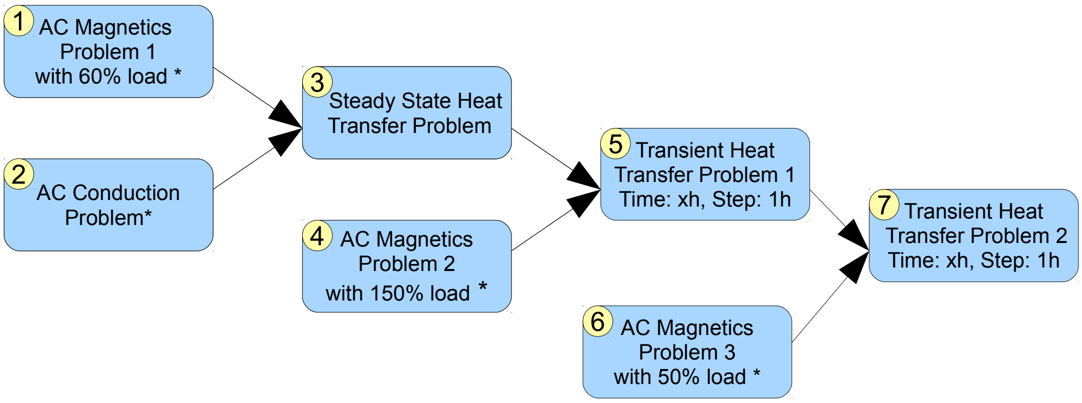

Figure 8.11: Step diagram for calculating transient problems with QuickField (optional)*

The blocks denoted with * in Figure 8.10 are optional. Another way to simulate this problem is to use one steady state heat transfer problem linked to a transient heat transfer problem 1 which can then be linked to transient heat transfer problem 2. In this case the volume powers of the insulation and the conductors must be calculated with formula 8.2 and 8.3 respectively for each step and edited directly in the block labels. The results are similar for both methods.

The data required for the block labels in transient heat transfer problems are listed in Table 8.26 below:

Table 8.26 Block label parameters in transient heat transfer problem

	Volume Power of the Heat Source [W/m^3]	*Thermal Conductivity [W/Km]*	*Thermal Capacity C[J/kgK]*	*Material Density ρ[Kg/m^3]*
Air	0	0.03	0	0
Soil 1	0	λ(T)	1000 (2)	1600
Conductor (Cu) (1,2,3)	0 or Q_c (1)	400	385	8920
Inner insulation (XLPE)	0 or Q_i (1)	0.28	1700	920
Outer insulation (PE)	0	0.38	1700	920
Screen (Cu)	0	400	385	8920

1) Indicates that the data depends on the simulation path chosen by the user. For transient heat transfer problems which have a link to AC magnetics and AC conduction problem, the value of the volume power must be set to zero, and for transient transfer problems without links to

AC magnetics and AC conduction problems the volume power value for the conductors and insulation must be calculated manually.

2) Indicates that the soil parameters depend on its properties, and can be different if a two zone model of the soil is taken.

8.5.2 *Results*

- Single trefoil formation

Figure 8.12 shows the time-temperature plot for single trefoil formation buried at 1.2m and first loaded with 60% of the maximum continuous load (calculated in the previous examples) to 150% transient load and to 50% of the maximum continuous load. After approximately 15h the hottest conductor reached the maximum allowed temperature of 90°C. After this the conductor load was decreased and after approximately 15h it reaches its starting temperature of 42°C.

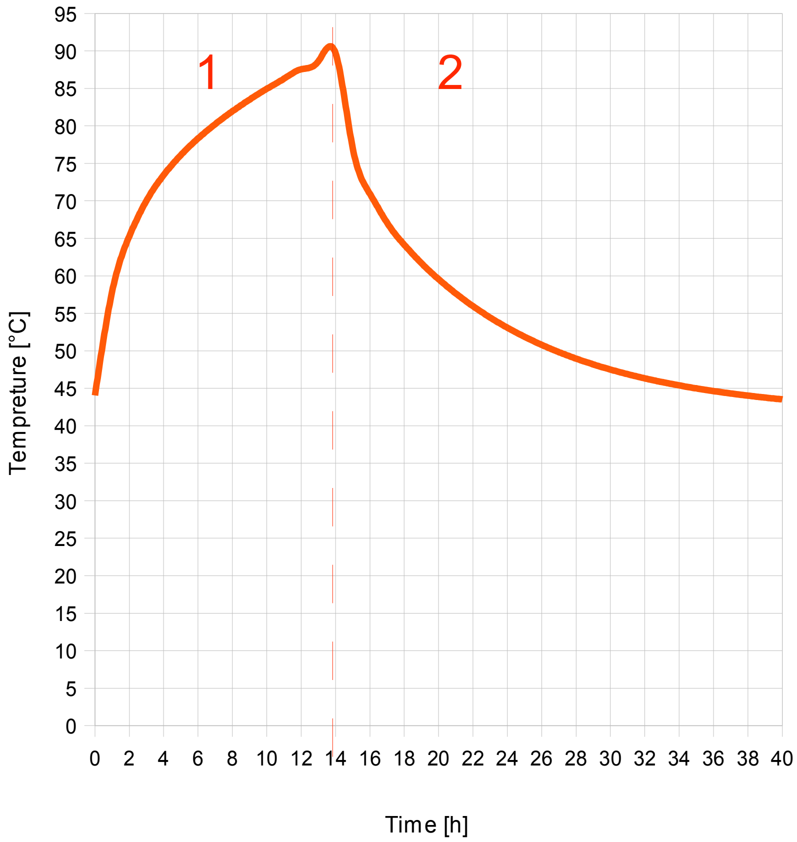

Figure 8.12: Time-temperature plot of trefoil formation buried at 1.2m with transient load

The first part of the graphic for the time-temperature plot represents the data retrieved from the transient heat transfer problem 1 from the starting point (T=42°C) until the point where the hottest conductor reaches 90°C (in this case t=15h). The second part of this plot represents the data retrieved from the transient heat transfer problem 2 from the starting point (T=90°C) until the point, where the temperature of the conductor reaches 42°C.

- Single flat formation

The same method was used for the flat formation. Figure 8.13 shows the time-temperature plot for single flat formation buried at 1.2m. The starting point was the temperature of the conductor loaded with 60% continuous load: 44°C. Then the conductor was loaded with 150% of the maximum continuous load until the temperature of the hottest conductor reached 90°C – this happens after approximately 14h. Afterwards the conductor was loaded with 50% of the maximum continuous load, and the conductor reaches its starting temperature after approximately 16h.

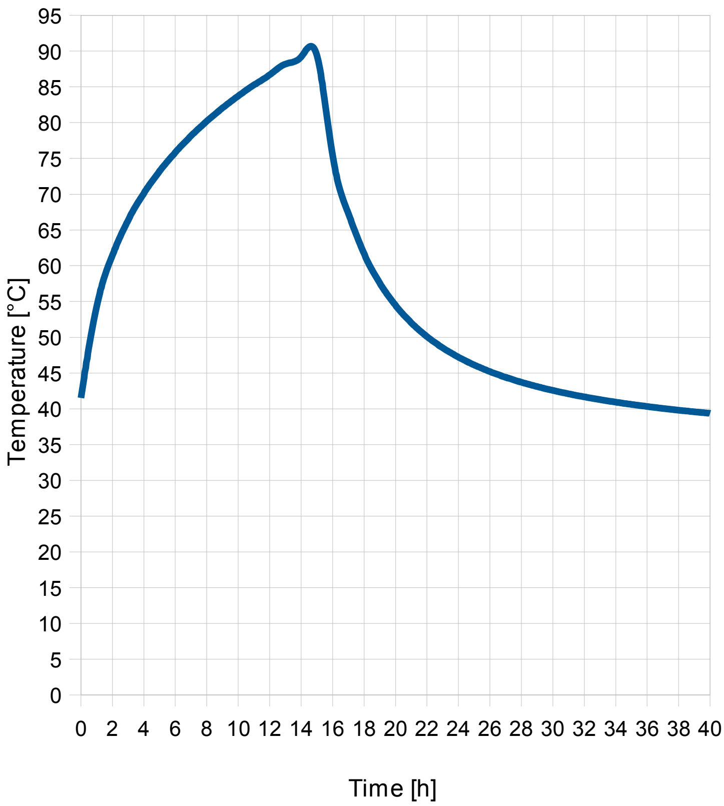

Figure 8.13: Time-temperature plot of flat formation buried at 1.2m with transient load

8.6 *Estimating the Power Transfer at Different Laying Depths for Single Trefoil Formation and Single Flat Formation.*

8.6.1 *Required data*

Every time the conductor formation is laid 0.5m deeper and it maximum continuous current load is calculated as described in point 8.2. The deepest point for this calculation is 11m. The results for each laying depth are then placed in a table and the power transfer/laying depth graphic is generated using Open Office.

8.6.2 *Results*

The curves in Figure 8.13 represent the power transfer ratings at different depths for single trefoil and flat formation with the same physical and geometrical parameters for uniform soil thermal conductivity of 1W/Km (pulled lines) and for partial drying out of the soil (dashed lines). The soil is represented with the simple two zone approximation model discussed earlier.

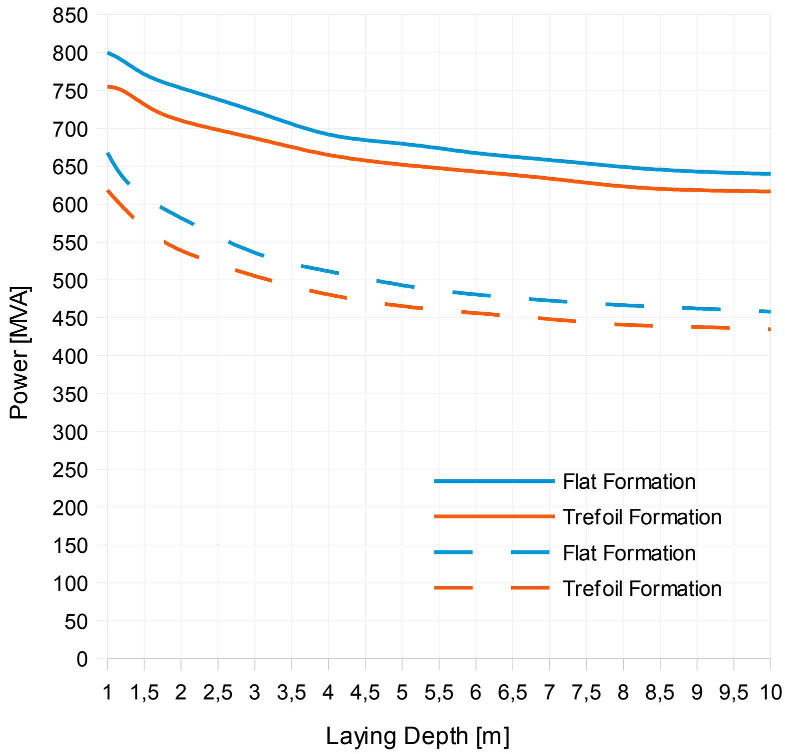

Figure 8.14 Power transfer/laying depth for single trefoil and flat formation

8.6.3 *Discussion of the results*

The deeper the cable system is laid the harder it becomes to transfer heat since the heat can dissipate only towards the surface of the ground. This is why the power transfer falls proportionally to the laying depth. But after a certain depth is reached, the heat dissipation speed stays the same even for greater depths because then the area can be viewed as an endless soil region. That is why the power transfer reaches a point where the laying depth no longer has an influence on the transfer rate. Cables laid in a dry soil have much lower power transfer ratings than the same cables laid in a soil where only partial drying out occurs. This example shows the importance of estimating the soil properties and the laying depth in order to design cables for the required power transfer ratings.

9 Summary

In this study the power transfer ratings, temperature fields and magnetic fields for high voltage XLPE power cables was investigated for different laying configurations and at different laying depths with the FEA software package QuickField. The results obtained with QuickField for permissible currents ratings at continuous load for buried cables in trefoil formation are confirmed with results obtained using the IEC 60 287 standard.

The theoretical part of the theses describes the underground XLPE cables basic design, its electric and dielectric losses and its thermal model. It includes the IEC 60 287 standard formulas for calculating the thermal resistance for different underground cable configurations, and also the IEC 60 287 standard formulas for calculating the permissible currents ratings for buried cables. Furthermore there is a brief description of the possible biological effects caused by alternating magnetic fields and some prescribed limits for these fields.

The practical part of the paper includes a short description of the QuickField models which were used for solving problems in this study. Several examples show how to use QuickField in order to estimate current ratings for continuous and transient loads at different laying depths and for different soil properties, magnetic fields, electric and dielectric losses of high voltage underground cables. A 500kV single core XLPE cable with copper wire screen with stranded compacted conductors in trefoil and flat formation was used for the models.

This study was made in order to show the high potential of the FEA program QuickField for designing optimal underground cable systems and calculating different cable parameters. It has a very user friendly interface and the results can be obtained as field pictures, graphics and tables.

10 Index

10.1 References

[1] I.Preis; Thermische Belastbarkeit von erdverlegten Mittelspannungskabeln; Institut für elektrische Anlagen und Hochspannungstechnik der Technische Universität Graz; Diplomarbeit Sept. 2003

[2] NKT Cables Catalog; High Voltage Cable Systems; Cable and Accessories up to 550kV

[3] Harry Orton; Long life XLPE- insulated Power cables

[4] Kupfer in der Elektrotechnik-Kabel und Leitungen; Deutsches Kupfer Institut Auskunfts- und Beratungsstelle für die Verwendung von Kupfer und Kupferlegierungen; Düsseldorf; 2000; http://www.kupfer-institut.de

[5] Hans J.Mair; Kunststoffe in der Kabeltechnik; Kontakt & Studium; Band 111

[6] L. Heinhold, R. Stubbe; Kabel und Leitungen für Starkstrom; MCD Verlag, Einlagen; 1999; ISBN 3-89578-088-X

[7] R.Woschitz; Hochspannungsleitungen; Institut für elektrische Anlagen und Hochspannungstechnik der Technische Universität Graz; Vorlesungsskriptum WS2002/2003

[8] Wikipedia; Joule Heating; http://en.wikipedia.org/wiki/Joule_heating

[9] Wikipedia; Skin Effect; http://en.wikipedia.org/wiki/Skin_effect

[10] Thomas Worzyk; Submarine Power Cables: Design, Installation, Repair, Environmental Aspects; Springer-Verlag; 2009; ISBN 978-3-642-01270-9

[11] IEC 60 287-1-1 standard; Electric cables-calculation of the current rating-Part 1; International Electrotechnical Commission, 1994

[12] IEC 60 287-2-1 standard; Electric cables-calculation of the current rating-Part 2; International Electrotechnical Commission, 1994

[13] Norbert Leitgeb; Machen Elektromagnetische Felder krank?; Springer-Verlag Wien New York; 1990;ISBN-3-211-83420-6

[14] Tera Analysis; QuickField User's Guide 5.2; Copyright 2004; http://www.quickfield.com

[15] Marlene Marinescu; Elektrische und Magnetische Felder. Eine praxisorientierte Einführung; Springer ISBN 978-3-642-24219-9

10.2 *Symbols*

R_{AC}	conductor ac resistance at maximum operating temperature [Ω/m]
R'	conductor dc resistance at maximum operating temperature [Ω/m]
y_s	skin effect factor
y_p	proximity effect factor
f	supply frequency [Hz]
x_s	argument of Bessel function used to calculate skin effect
k_s	skin effect coefficient
x_p	argument of Bessel function used to calculate proximity effect
d_c	diameter of conductor [mm]
s	distance between conductor axes [mm]
k_p	proximity effect coefficient
R_0	conductor dc resistance at 20°C [Ω/m]
α_{20}	temperature coefficient of electrical resistance at 20°C
Θ	maximum operating temperature
P_i	total current dependent losses per m [W/m]
n	number of conductors
R_i	resistance of a 1 m piece of cable insulation [Ω/m]
ω	angular frequency of the AC voltage ω=2πf [Hz]
C	cable capacitance per unit length [μF/km]
D_i	diameter of the insulation [m]
d_s	diameter of the conductor screen [m]
ε	dielectric constant of the insulation material
U_0	voltage to earth [V]
T_1	thermal resistance per core between conductor and sheath [Km/W]

T_2 thermal resistance between screen and armour [Km/W]

T_3 thermal resistance of the outer insulation [Km/W]

T_4 soil thermal resistance [Km/W]

ρ_T thermal resistivity of material [Km/W]

t_1 thickness of the insulation between conductor and screen [mm]

t_3 thickness of serving (outer insulation) [mm]

D'_a external diameter of the armor (screen) [mm]

L distance from the surface of the ground to the cable axis [mm]

D_e external diameter of one cable [mm]

s_1 axial separation between two adjacent cables [mm]

I current flowing in one conductor [A]

$\Delta\Theta$ permisible temperature rise of conductor above the ambient temperature [K]

R alternating current resistance per unit length of the conductor at maximum operating temperature [Ω/m]

W_d dielectric loss per unit length for the insulation surrounding the conductor [W/m]

n number of load-caring conductors in the cable (conductors of equal size and carrying the same load

λ_1 ratio of losses in the metal sheath to total losses in all conductors in that cable

λ_2 ratio of losses in the armouring to total losses in all conductors in that cable

υ ratio of the thermal reactivities of dry and moist soil ($\upsilon=\rho_d/\rho_w$)

ρ_d thermal resistivity of the dry soil [Km/W]

ρ_w thermal resistivity of the moist soil [Km/W]

$\Delta\theta_x$ critical temperature rise of the soil. i.e the temperature rise of the boundary between the dry and the moist zones above the ambient temperature of the soil [K]

θ_x critical temperature of the soil and the temperature of the boundary between dry and moist zones [^{o}C]

θ_a	ambient temperature [ºC]
P_L	power losses in the conductor [W/m]
Q_i	volume power of the insulation [W/m^3]
Q_c	volume power of the conductor [W/m^3]
tan δ	loss angle
A	surface area of the conductor [m^2]
g	electrical conductivity [S/m]

12.2 Pictures

Figure 2.1: XLPE cable design.[2]......5
Figure 2.2: Conductor forms [6]......7
Figure 3.1: Skin effect [9]......13
Figure 3.2: Loss tangent diagram [6]......18
Figure 4.1: Thermal equivalent circuit for underground cable [6]......20
Figure 4.2: Temperature distribution at a maximum continuous load for trefoil formation......23
Figure 4.3: Flat formation with equal phase distances......24
Figure 6.1: Eddy currents induced by alternating magnetic field in the human body [13]......30
Figure 7.1: Block labels in AC magnetics problem [14]......37
Figure 7.2: Edge labels in AC magnetics problem [14]......39
Figure 7.3: Block labels in AC conduction problems [14]......40
Figure 7.4: Edge labels in AC conduction problems [14]......41
Figure 7.5 Block labels in heat transfer problems [14]......42
Figure 7.6: Edge labels in heat transfer problems [14]......43
Figure 7.7: Fine mesh automatically generated by QuickField with added artificial vertices in the region of interest......45
Figure7.8: Coarse mesh automatically generated by QuickField without added artificial vertices......45
Figure 7.9 Magnetic field above 500kV underground cable buried at 1.2m depth simulated with course mesh and with nonuniform fine mesh......46
Figure 8.1: NKT cables' data for 500kV single core XLPE cables with copper wire screen and APL sheath[2]......49
Figure8.2: NKT cables' data for soil thermal resistivity, laying depth and axial distance between phases and circuits [2]......49
Figure 8.3:Current density distribution in trefoil formation with solid conductors......52
Figure 8.4:Current density distribution in trefoil formation with stranded conductors......52
Figure 8.5: Step diagram for estimating the maximum continuous current load......53
Figure 8.6: Geometry of the cable in trefoil formation simulated using QuickField......55
Figure 8.7 Thermal soil conductivity as function of temperature......57
Figure 8.8: Magnetic fields above 500kV underground cables buried at 1.2m depth, loaded with 1000A......61
Figure 8.9: Magnetic fields measured at ground level (red) and 0,5m above ground (green) for two flat formations at 1000A load and 1.2m laying depth......62
Figure 8.10: Step diagram for estimating the maximum current load at continuous mode......64
Figure 8.11: Step diagram for calculating transient problems with QuickField (optional)*......71

Figure 8.12: Time-temperature plot of trefoil formation berried at 1.2m with transient load.........................72
Figure 8.13: Time-temperature plot of flat formation buried at 1.2m with transient load..............................73
Figure 8.14: Power transfer/laying depth for single trefoil and flat formation..75

12.3Tables

Table 1: Physical characteristics of aluminium and copper (data referenced to copper at 100) [3]................6
Table 2:Properties of cable insulation [5]...8
Table 3.1 Skin effect and proximity effect coefficients [11]...15
Table 6.1: Prescriptive limits for 50 Hz alternating magnetic fields [13]......................................34
Table 8.1: Cable geometrical parameters..50
Table 8.2: AC magnetics problem parameters for cable with solid conductors.............................51
Table 8.3: AC magnetics problem parameters for cable with stranded conductors.......................51
Table 8.4: Power losses per conductor..52
Table 8.5: Cable's geometric parameters...54
Table 8.6: AC magnetics problem block label's parameters 56
Table 8.7: Steady state heat transfer problem block label parameters 57
Table 8.8: Edge label values for steady state heat transfer problem..58
Table 8.9: Power losses...58
Table 8.10: Current ratings/ power ratings 58
Table 8.11 Current ratings/power ratings for trefoil formation...59
Table 8.12: Required block label values for cable simulated in AC magnetics problem 60
Table 8.13: Block label values for steady state heat transfer problem...63
Table 8.14: Edge labels values 64
Table 8.15: Block label parameters for AC conduction problem..65
Table 8.16: Edge label parameters for AC conduction problem...65
Table 8.17: Block label parameters for steady state heat transfer problem....................................66
Table 8.18: Edge label parameters for steady state heat transfer problem.....................................66
Table 8.19: Block label parameters for AC magnetics problem...67
Table 8.20: Block label parameters in steady state heat transfer problem.....................................67
Table 8.21: Edge label parameters for steady state heat transfer problem.....................................68
Table 8.22: Maximum current ratings/ power ratings for soil temperature of 15ºC......................................68
Table 8.23: Maximum current ratings/ power ratings for soil temperature of 20ºC.....................................69
Table 8.24: Maximum current ratings/ power ratings for trefoil formation (one circuit)..............................69
Table 8.25: Maximum current ratings/ power ratings for trefoil formation (one circuit)..............................70
Table 8.26 Block label parameters in transient heat transfer problem...71

EIDESSTATTLICHE ERKLÄRUNG

Ich erkläre an Eides statt, dass ich die vorliegende Arbeit selbstständig verfasst, andere als die angegebenen Quellen/Hilfsmittel nicht benutzt und die den benutzten Quellen wörtlich und inhaltlich entnommenen Stellen als solche kenntlich gemacht habe.

Graz, am 19.10.2012 ....

....
(Unterschrift)

Englische Fassung:

STATUTORY DECLARATION

I declare that I have authored this thesis independently, that I have not used other than the declared sources / resources and that I have explicitly marked all material which has been quoted either literally or by content from the used sources.

19.10.2012
....
date

....
(signature)